https://ntrs.nasa.gov/search.jsp?R=19820013163 2020-03-21T08:46:52+00:00Z

NASA
TP
1976
c.1

NASA
Technical
Paper
1976

March 1982

TECH LIBRARY KAFB, NM
0068146

# Fluctuating Pressures on Fan Blades of a Turbofan Engine

## *Static and Wind-Tunnel Investigations*

LOAN COPY RETURN TO
AFWL TECHNICAL LIBRARY
KIRTLAND AFB, N. MEX.

James A. Schoenster

16 APR 1982
Technical Library
AF Weapons
Laboratory

NASA

TECH LIBRARY KAFB, NM
0068146

**NASA Technical Paper 1976**

1982

# Fluctuating Pressures on Fan Blades of a Turbofan Engine

## *Static and Wind-Tunnel Investigations*

James A. Schoenster
*Langley Research Center*
*Hampton, Virginia*

NASA
National Aeronautics and Space Administration

**Scientific and Technical Information Branch**

Use of trade names or names of manufacturers in this report does not constitute an official endorsement of such products or manufacturers, either expressed or implied, by the National Aeronautics and Space Administration.

## SUMMARY

As part of a program to investigate the fan noise generated from turbofan engines, miniature pressure transducers were used to measure the fluctuating pressure on the fan blades of a JT15D engine. Tests were conducted with the engine operating on an outdoor test stand and in a wind tunnel. Techniques used for interpreting these measurements included both narrow-band spectral analyses and signal enhancement analyses using a precise measurement of the blades circumferential position as a reference. The measured results were used to identify the noise generating mechanisms at the fan face. It was found that a potential flow interaction between the fan blades and six, large support struts in the bypass duct is a dominate noise source in the JT15D engine. Pressure measurements on the fan blades showed the effect of inlet turbulence during static tests and the changes which occurred when forward speed was included in the tunnel. Effects of varying the fan speed and the forward speed on the blade pressure are also presented.

## INTRODUCTION

For several years, studies have been conducted to understand the mechanism of noise generated by the fan of a turbofan engine. Results from these studies demonstrated that measurements obtained from ground static tests were not representative of the noise measured in flight tests (e.g., ref. 1). It was found that several mechanisms are involved in the noise generation process and that one mechanism may dominate under one test condition while another mechanism dominates during a different test condition. Relatively early in these studies, airflow drawn into the engine from ground static tests was observed to be significantly more turbulent than that existing in flight (ref. 2). Some of this turbulence was caused by the test stand supporting the engine; some was a result of the engine's proximity to the ground; and some exists naturally in the atmosphere and is drawn into the inlet. These increased levels of turbulence caused the ground tests to yield much higher levels of noise than those obtained in flight. Several other mechanisms which were common to flight and ground conditions were identified as potential sources, such as rotor/boundary-layer interaction, rotor-alone noise, rotor/bypass-stator noise, and rotor/core-stator noise. To aid in understanding the complex mechanisms of fan noise generation and to quantify the differences in the inflow encountered by the engine under static tests and during flight, knowledge of the loading on the fan blades is necessary. Hanson (refs. 3 and 4) developed a unique data acquisition/reduction method which helped to identify some of the potential noise generating mechanisms. Miniature pressure transducers were mounted on the blades of the fan and the data from these transducers were analyzed as functions of position around the circumference, making it possible to obtain a "map" of the fluctuating pressures at the fan face. Although a direct application of these measurements to predict noise generation has not yet been established, several characteristics of the noise mechanisms may be identified. Studies using these techniques have been reported by Rogers and Ganz (ref. 5) and by Ganz (ref. 6). Fan-blade pressure data from a large turbofan engine were used to interpret noise mechanisms during static ground tests, flight tests, and a static ground test using an inflow control structure (ICS). These results indicate that large turbulent inflow during static tests caused noise levels above those encountered in flight.

In view of the large differences in the radiated sound field between ground static tests and actual flight conditions, it became apparent that reliable ground-test methods to simulate actual flight conditions must be developed. In a cooperative effort among NASA research centers, a program was established to study, in detail, methods to improve simulated flight conditions during ground tests. At Lewis Research Center (refs. 7, 8, and 9), ground static tests have been conducted using various configurations of a modified JT15D engine. Measurement results included far-field acoustic data, effects of modifying the inflow conditions, and effects of inflow control structures on the noise generated by the fan. At Langley Research Center, ground static tests and wind-tunnel flight-simulation tests have been conducted and flight tests on the same engine are currently being conducted. A comparison among these three sets of results is expected to provide the needed information on the improvement of simulated flight-test methods on fan noise. The ground tests were performed on the static test stand at NASA Ames Research Center, and the flight-simulation tests were conducted in the Ames 40- by 80-Foot Wind Tunnel. The measurements in these two tests included far-field noise and extensive fan-blade fluctuating pressure, obtained from fan-blade-mounted transducers (FBMT's). Far-field data and some preliminary FBMT data were presented in reference 10.

The purpose of this report is to provide a more extensive analysis of the FBMT data from the JT15D turbofan engine. FBMT measurements obtained from a static test stand and in a wind tunnel are presented. The experimental results are discussed in terms of narrow-band spectrum, space/time histories, the mean of the deviation and standard deviation, and the harmonic order analysis.

## SYMBOLS

$f_n$ fan rotational frequency, Hz

N total number of fan revolutions

P pressure, Pa

$\Theta$ total number of discrete, angular, fan-blade positions

$\sigma$ standard deviation of pressure, Pa

Subscripts:

n number of fan revolutions

$\theta$ angular position around inlet circumference, deg

Abbreviations:

ccw counterclockwise

FBMT fan-blade-mounted transducer

FFT fast Fourier transform

freq frequency

ref reference

A bar ($\bar{}$) over a symbol denotes the mean value.

## DESCRIPTION OF EXPERIMENT

### Test Engine

The test engine, a modified JT15D turbofan,[1] is a twin-spool, front-fan jet propulsion engine which has a full-length annular bypass duct. It has a nominal bypass ratio of 3.3 and a maximum thrust capability of 9790 N. (See table I for specifications.)

The fan is 53.3 cm in diameter and has 28 blades. (See figs. 1 and 2.) The fan is followed by a stator assembly consisting of a bypass stator which has 66 vanes and a core stator which has 71 vanes. The latter is the only major difference between a production JT15D engine (which has 33 core-stator vanes) and the test engine. The modified core stator has more blades and is aft of the rotor blade root a distance of 0.63 fan-blade root chord (compared to 0.28 chord for a production engine) so that the fan rotor/core-stator interaction tone was acoustically cut off and the broadband noise was diminished. The next rotating blade assembly is the compressor which is a combination axial-centrifugal compressor having 16 blades in the leading axial part of the unit.

As shown in figure 3, the engine core is supported by six internal struts which are located in the intermediate case of the engine. These supports traverse the compressor and bypass ducts to attach the core to the outer wall of the engine intermediate case. As shown in figure 2, these struts are located behind the stator assembly.

The test engine was fitted with a muffler to reduce the aft-radiated noise from the bypass duct. This was considered necessary to minimize any possible contamination of the measurements of front-radiated fan noise of interest in the present investigation. The muffler was designed so that the bypass and core exit areas remained the same as in an untreated engine.

### Test Facilities and Setup

Outdoor test stand.- The engine was mounted outdoors on a single strut 4.57 m above the ground, and the engine was encased in a nacelle with the exception of one section on the bottom side. (See fig. 4.) Microphones for far-field measurements (a traversing microphone supported on a rail and pole microphones) were placed no closer than 4.05 m from the fan face of the engine. A concrete pad supports the entire setup. This test setup presents a minimum of flow distortion into the engine inlet resulting from the support structure, the ground plane, or the instrumentation supports.

---

[1]Manufactured by Pratt & Whitney Aircraft of Canada.

Wind tunnel.- The same mounting strut used in the outdoor test was used to install the engine in the Ames 40- by 80-Foot Wind Tunnel (fig. 5). The test-section floor and walls in the immediate area surrounding the engine were lined with a 7.62-cm-thick layer of acoustic foam. Far-field microphones similar to those used outdoors were mounted around the engine. During the wind-tunnel tests, the entire nacelle was in place. Tests were conducted for conditions ranging from the tunnel off to a simulated forward speed of 44 m/s. With the tunnel off, the operation of the engine induced a flow in the tunnel test section; however, the maximum induced speed was less than 6 m/s.

Test conditions.- Data obtained on the outdoor test stand were at nominal fan speeds from 6750 to 13 490 rpm. To allow for stable engine operation (constant engine speeds), tests were conducted only when the speed of the prevailing wind was less than 3 m/s.

For the wind-tunnel tests, data were obtained for several combinations of fan speed and tunnel speed. For purposes of comparison with the outdoor tests, results were obtained at a fan speed of 6750 rpm with a tunnel speed of 44 m/s. To study the effect of fan speed on the blade pressure fluctuations, the tunnel was turned off and the fan speed was slowly varied from 12 800 to 8450 rpm while data were continuously recorded. The effect of flight speed was studied by keeping a steady fan speed at 10 500 rpm and acquiring data with the tunnel off and at tunnel speeds of 10, 31, and 44 m/s. Temperature was about 17°C (62°F) during the outdoor tests and about 19°C (67°F) in the wind tunnel. Adjusting the fan speed for temperature effects would result in a difference of less than 1 percent between the outdoor and wind-tunnel tests, and therefore, actual speeds are used in this paper.

## Instrumentation and Data Processing

Fan-blade-mounted transducers.- Miniature (1-mm diam) pressure transducers were bonded to the blade surface at three locations along the span (fig. 6). The total thickness of the mounted transducer was less than 0.33 mm above the surface of the blade including the rubberized bonding material which was used to fair the transducer to the curvature of the blade. Based on an evaluation of this mounting arrangement (ref. 11), the addition of the transducers to the blade is not expected to have a significant effect on the pressure field being investigated in this study. A photograph of the installation is presented in figure 7. Signals from these transducers were transmitted from the fan hub to an antenna in the inlet duct wall and recorded on magnetic tape as analog pressure signals (fig. 8). The system was designed to measure pressures in the range of 20 Hz to 20 kHz with a sensitivity of 0.145 mV/Pa (1 V/psi). The systems signal to noise ratio is 50 dB and the dynamic range is from 120 to 170 dB. Details explaining the data acquisition system for these transducers may be found in reference 12.

Data processing.- Data from the fan-blade-mounted transducers presented in this paper were analyzed by one of two methods. The first method for analyzing data from the fan-speed sweep test uses an on-line spectrum analyzer having a 10-Hz nominal bandwidth of analysis up to 5000 Hz and a three-dimensional display generator. Each spectrum represents 256 averages, and as the fan speed is varied, each subsequent averaged spectrum is displaced on the plot to yield a stepped time history of the spectra. Sixteen independent spectra are presented, covering a fan speed of 12 800 to 8450 rpm. The change in fan speed during any one averaging time is about 5 Hz, or half the bandwidth of analysis.

The second data analysis method follows a procedure developed by Hanson (ref. 4) to analyze data from transducers on rotating machinery. Applications of this method were made in references 4, 5, 9, 10, and 13. The method relates the measured pressure signal from the FBMT with a precise measurement of the fan-blade position. This allows the data to be evaluated in terms of the angular position of the blade-mounted transducers. Thus, the measured pressure is analogus to the measurements of a continuous circular array of fixed transducers. The blade-position sensor incorporates an optical sensor system which is triggered each time a selected polished blade passes the sensor. This signal is converted into a 2-ms constant-amplitude pulse whose rising slope indicates the passing of the polished blade. This signal is recorded along with the pressure data, and for this test, the sharp rising slope provides an accurate indication that the instrumented blade is at the top-center position of the engine inlet. Additional details of this system may be found in reference 12.

With the pulsed signal as a reference, the pressure data are digitized at a rate of 360 points per revolution (independent of the fan speed). These digitized data are then processed through a fast Fourier transform (FFT) analysis program which provides a spectrum in bandwidths of $0.35f_n$, where $f_n$ is the fan rotational frequency. This is the spectrum of the overall pressure variation on the rotating blade.

The data are then ordered in the form $P_{n,\theta}$ where $n$ is the number of the fan revolution (established from an arbitrary starting point) and $\theta$ is the number of the data point in a revolution (representing the angular position around the inlet circumference at which the measurement was obtained).

The mean value of the total data sample $P$ is calculated by

$$\bar{P} = \frac{1}{N\Theta} \sum_{n,\theta=1}^{N,\Theta} P_{n,\theta} \tag{1}$$

where $N$ and $\Theta$ were selected to be 1000 and 360, respectively. This value is subtracted from all the data points (i.e., $(P_{n,\theta} - \bar{P})$). The adjusted values of $P_{n,\theta}$ are then plotted on a scale of revolution number $n$ versus angle for each revolution $\theta$ to form a space/time history of the fluctuating pressure measured on the blade surface.

The next step is to calculate the mean value of the deviation (called mean value analysis in this paper) $P_\theta$ and the standard deviation $\sigma_\theta$ of the pressure signal as a function of angular position by using the following formulas:

$$P_\theta = \frac{1}{N} \sum_{n=1}^{N} (P_{n,\theta} - \bar{P}) \qquad (N = 1000) \tag{2}$$

$$\sigma_\theta = \left[ \frac{1}{N} \sum_{n=1}^{N} (P_{n,\theta} - P_\theta)^2 \right]^{1/2} \qquad (N = 1000) \tag{3}$$

These values are plotted as functions of blade angle.

The last step in this process is to divide the data points into four 250-revolution increments, average the data, and order the data points to form a single

sequence of 1440 data points. A Fourier analysis of this sequence yields a spectrum of the enhanced pressure in terms of the harmonics of the fan speed. The effective bandwidth is $0.25f_n$.

Variations in the mean value of the deviation indicate a mechanism causing a deterministic spatial change in the static pressure around the circumference. The standard deviation is a measure of the magnitude of pressure fluctuations, either periodic or random, on the blade surface at a fixed angular position. A constant standard deviation around the entire circumference indicates uniform fluctuations over the entire inlet, while variations in standard deviation around the circumference indicate that there is a mechanism causing a spatial distribution of the time-varying pressure levels over the inlet. A comparison of the spectral analysis of the total signal to that of the enhanced signal provides a measure of the amount of pressure fluctuation which is harmonically related to the fan speed, thereby separating the periodic component from the random component.

Demonstration of the data analysis method.- A diamond-shaped rod was mounted about 3 cm in front of the fan face of the JT15D engine at 220° around the circumference from top center of the inlet. This rod provided a disturbance at a known, fixed location for the FBMT's to detect. Shown in figure 9(a) is the space/time-history plot for 500 revolutions of the engine during an engine run at 6710 rpm. A disturbance appears in the time history at 220° indicating the wake shed by the rod. It remains constant in location for all the fan revolutions. In figure 9(b), the mean value deviation and the standard deviation of the measured blade pressure are shown. The mean value deviation varies around the circumference with a large negative pressure followed by a large positive pressure at the location of the rod. The standard deviation shows no effect because of circumferential location, except for a significant increase at the location of the rod. These data indicate that the wake shed by the rod causes an increase in the steady pressure levels and in the random pressure fluctuations on the blade. The overall spectral analysis is shown in figure 9(c). A large-amplitude signal may be observed at the fundamental fan frequency (112 Hz) and at several harmonics up to about 6 kHz. Above 6 kHz, some peaks may still be observed; however, these peaks are generally not harmonics of $f_n$. The harmonics are at least 3 dB above the broadband noise level for this bandwidth of analyses (39 Hz). In figure 9(d), the enhanced-signal spectrum is presented. The spectrum shows the amplitude of the periodic pressure components as a function of harmonic order of the fan rotational frequency (in this test, 112 Hz). By comparing the enhanced-signal spectrum with the overall spectrum, components which are primarily periodic may be determined. For example, the components at $f_n$, $2f_n$, and $6f_n$ are primarily periodic with the rod in place, (i.e., the enhanced pressure level is within 1 dB of the fluctuating pressure level). These results indicate that, with the data processing method used, deterministic flow-field distortions can be identified up to the first few harmonics of the fan speed.

It should be noted, however, that examination of all four types of test results, as shown in figure 9, have been proven to be most instructive in identifying the characteristics associated with the engine, the test setup, and/or the test conditions.

## RESULTS AND DISCUSSION

### Outdoor Static Tests

The outdoor static tests were performed with the test stand shown in figure 4. Tests were made only when the prevailing winds were less than 3 m/s to minimize variation in the fan speed because of the wind.

At a nominal fan speed of 6750 rpm, the space/time-history plots (fig. 10) for transducers G, H, and I (shown in fig. 6) show no observable trends or characteristics. This implies that there is no strong deterministic flow distortion in front of the fan face. Plots of the mean value deviation and the standard deviation for this test are shown in figure 11. A quasi-sinusoidal variation of one cycle around the circumference is observable at all three transducer locations along the blade span, while a mean value variation of six cycles around the circumference is clearly seen in FBMT G. (There is also some indication of this variation in FBMT H and I.) The observed one-cycle variation differs from that shown in the sample, in that the sample shows a sharp peak at one location, figure 9(a), while the observed variation in figure 10 appears to be changing smoothly over the entire circumference. The standard deviation plot for all three transducers shows a relatively constant level around the circumference of the inlet.

The spectral plots of the overall pressure (fig. 12) show large peaks, as expected, at the fundamental fan frequency (the one-cycle variation) and at the sixth harmonic (the six-cycle variation) on all three spanwise transducers. In addition, all the peaks in the range below 4 kHz may be identified with harmonics of the fan rotational frequency. The peaks above 4 kHz, however, are not harmonically related to the rotational frequency of the fan. Shown in figure 13 is the level of the enhanced signal for 90 harmonic orders. At the first, second, and sixth harmonics of the rotational frequency, the signals from FBMT H and I are predominately periodic (the overall level and the enhanced-signal level are about equal), and for FBMT G, the first and sixth harmonics are predominately periodic. At all other frequencies, the enhanced-signal level is considerably lower than the overall level, indicating a predominately random signal. A comparison of this enhanced-signal spectrum to the enhanced spectrum of the sample (fig. 9) shows that all the harmonic content is considerably higher with the rod. This holds true even though it was shown that the rod has a spatial effect over only about half the inlet.

The six-cycle pattern shown by the FBMT's has been observed before in the JT15D engine (e.g., ref. 9). This pattern is attributed to an effect caused by six large struts in the bypass duct (fig. 3). Prior to the use of fan-blade-mounted transducers, the existence of this pressure pattern was unsuspected (e.g., ref. 14). The potential flow interaction of the 6 struts with the 28 fan blades can excite a spinning mode with 22 nodes in the duct. Directivity patterns measured in the far field at 10 500 rpm (ref. 9) and 12 000 rpm (ref. 10) indicate that this particular spinning mode has been excited and radiates to the far field. Therefore, the potential flow interactions between fan blades and the six struts is a dominant source of fan noise.

The space/time history for a 13 490-rpm run is shown in figure 14. During this run, large random variations may be seen in the pressure signals from all three spanwise transducers. Although some of these variations last only for a few cycles and traverse across angular locations, all three transducers show a large concentration of disturbances between 150° and 240°. These disturbances are not steady, they continue throughout the data run. The standard deviation for all three transducers

(fig. 15) shows these effects as an increase in level between 150° and 240°. Only FBMT G still shows the six-cycle variation per revolution in the mean value analysis, with FBMT I and H showing no definable pattern.

The overall spectral plots (fig. 16) show a large increase in all the harmonics, and as indicated in the mean value analysis, the sixth harmonic is no longer as dominant in FBMT H and I as it was at 6750 rpm.

The disturbances that the blade transducers measure are caused by atmospheric turbulence, ground turbulence, and/or test-stand turbulence which are shown to exist in references 2, 3, 4, and 14. These data indicate that, because of the concentration of the disturbances at the bottom of the inlet (figs. 14 and 15), the fluctuations are the result of ground turbulence or test-stand turbulence. Prior studies would also indicate that the test stand is the more likely cause since the engine is mounted so far above the ground (7.5 fan diameters). Thus even though the test stand was about as structually small as practical, the winds at a minimum, and the engine a significant distance above the ground, turbulence at the fan face from all or some of these inputs was sufficient to be measured by the blade transducers. The noise generated as an effect of the environment could be sufficient to mask the noise generated by the engine without these effects.

## Wind-Tunnel Tests

Effect of engine speed.- Presented in table II is a listing of test conditions in the tunnel and the range of control of fan speed under these conditions. For the two speeds listed (12 000 and 10 500 rpm), it was observed that once there was a significant forward speed, 10 m/s, the fan speed could be held to within 0.25 percent of the set speed. In the tunnel without the forward velocity (induced flow caused by engine operation was less than 6 m/s), the fan speed varied two to three times as much as with forward velocity. The inability to hold the fan speed constant may have had an effect on the generation of fan tones. Although this speed variation was not investigated by this study, the response of the FBMT's to steadily varying fan speed was investigated. Shown in figure 17 are the results of slowly varying the fan speed from 12 800 to 8450 rpm. For this sweep run, the tunnel was off and the bandwidth of analysis was considerably narrower than that for the other plots in this report (10 Hz compared to 78 to 39 Hz). The harmonic amplitudes appear higher only because the narrow-bandwidth filter presents the broadband-pressure spectral measurements at a lower level. An overview of FBMT I (fig. 17(a)) shows three ranges. The first range is around 12 800 rpm, where all of the harmonics up to 5000 Hz are clearly visible above the broadband noise, although the sixth harmonic of the engine frequency is the largest peak. In this speed range, a large portion of the blade is moving at supersonic speeds. The next range is around 12 050 rpm, where the blade tip is operating in a transonic speed range. The spectra show a high broadband noise component which almost masks all the harmonic components, including the sixth harmonic. The third range is below 11 150 rpm, where the dominant components are the fundamental fan frequency and the sixth harmonic. Other harmonics are clearly observable, but at lower amplitudes. Results for FBMT H presented in figure 17(b) are similar to those of FBMT I. However, FBMT G (fig. 17(c)) does not have the three areas clearly separated. At this transducer location (refer to fig. 6), the blade does not go supersonic until about 14 000 rpm, although there is some increase in the levels of all the higher harmonics at 12 800 rpm. Also, while not as clear as that of FBMT H and I, the broadband level does increase at about 12 050 rpm, somewhat masking the harmonics. Below 12 050 rpm, the fundamental frequency and the sixth-harmonic components dominate the spectra, and all other harmonics are much lower in

amplitude. As noted in reference 9, it is very difficult to maintain the fan speed within 300 rpm when testing outdoors with no inflow control devices. The sweep spectral data shown indicate the loading on the blades varies considerably as the fan speed approaches supersonic velocity, and such variation could easily cause different noise generation mechanisms (refs. 3 and 15) to be triggered. This variation would make it very difficult, if not impossible, to separate the different mechanisms causing the noise.

Effects of tunnel speed.- Comparisons of data at various tunnel speeds are presented to show the effect of forward speed on the FBMT measurements. Shown in figure 18 are plots of the standard deviation and the mean value of FBMT I, H, and G for the engine, muffler, and traverse-support test condition at a fan speed of 10 500 rpm and a tunnel speed of 44 m/s. For these conditions, the six-cycle variation per revolution is clearly identifiable on all three transducers. Also as previously observed, there is no spatial variation of the standard deviation to angular location (i.e., the level is constant around the circumference). These plots look very similar to those obtained with the tunnel off. The only difference being the tunnel-off levels of the standard deviation are slightly higher.

The overall spectral plots for the three transducers are shown in figure 19 at a fan speed of 10 500 rpm for four tunnel speeds. It may be observed that harmonics of the fundamental fan frequency occur over the entire frequency range of the spectrum (fig. 19(a)) obtained by FBMT I with the tunnel off. With the increase in forward speed of the tunnel, many of the harmonics fall below the broadband level. The same occurrence may be observed in FBMT H (fig. 19(b)). However, the harmonics are not as visible in FBMT G (fig. 19(c)) and the differences in spectra among the tunnel speeds are much less. The peak in all transducers at 11 550 Hz for virtually all tunnel speeds has been identified with the 66 stator vanes in the bypass duct. While this interaction is not anticipated to be a source of noise (a cut-off mode, ref. 15) in the duct, it is reassuring to observe that the FBMT's are capable of detecting the presence of the stators.

In reference 10, it was shown that once the tunnel speed reached 10 m/s the sound power in the far field changed only slightly. It appears that the pressure loading on the blades, as measured by the FBMT, also is unchanged with tunnel speed once a significant flow in the tunnel is reached.

The enhanced-signal spectra (fig. 20), when compared to the overall spectra (fig. 19), show that the signals at the fundamental fan frequency, the 6th harmonic order, and the 66th harmonic order are primarily periodic. (See also table III.) For FBMT G under all configurations, the level does not vary more than 1 dB for the overall level and the enhanced-signal level is never more than 2 dB below the overall level. The same holds true for FBMT H. Only FBMT I (within the fan-duct boundary layer) differed, in that the overall level dropped 3 to 4 dB with increasing tunnel speed at the fundamental fan frequency. However, the signal is still primarily periodic, since the overall levels and the enhanced levels are within 1 dB of each other. The implication of this stability is that these signals are not dependent on inflow conditions but are inherent in the engine and that, for this engine-inlet configuration, no other mechanism was dominant enough to affect these measurements.

## Comparison of Outdoor Static Tests to Wind-Tunnel Tests

Analyses of data from FBMT G, H, and I during the tunnel tests with a simulated forward speed of 44 m/s (representative of all tunnel-on data) are presented in fig-

ures 21, 22, and 23. The standard deviation and the mean value analysis for FBMT G, H, and I at 6750 rpm look very similar to the outdoor results. (See figs. 11, 12, and 13.) The mean value analyses show the same one- and six-cycle-per-revolution variations as the outdoor test. The only observable difference is that the level of the standard deviation is about 10 percent lower in the tunnel. However, this small difference in the standard deviation is much more observable in the overall spectral plots, compare figure 22 with figure 12. Below 5000 Hz, all three transducers show a 4- to 5-dB drop in the broadband level compared to the data obtained on the outdoor test stand. Above 5000 Hz, the level drops 2 or 3 dB, although there is almost no change at some frequencies. In addition, the multiple harmonics, clearly visible in the outdoor tests, are now buried in the broadband spectra of the tunnel tests, even though this level is lower than before. The only signal levels still showing more than 6 dB above the broadband noise for all the spanwise measurements are the first and sixth harmonics. The enhanced-signal spectra (fig. 23) show that, although the first-harmonic periodic components have varied somewhat on all three transducers, the sixth-harmonic level has remained at almost the same amplitude in the tunnel and outdoors. This is consistent with the mean value plot observations.

The space/time-history analysis for the 13 460-rpm run in the tunnel showed no trend or observable pressure patterns, even with the tunnel off. The standard deviation and mean value plots (fig. 24) do not show any similarity with the outdoor tests (see fig. 15), even with the tunnel off. While there is an indication of the six-cycle variation per revolution in FBMT G, the general shapes are not at all similar. However, one phenomenon may be observed. The standard deviation (i.e., the random component), as in the tunnel at 6750 rpm, does not have any particular sensitivity to angular location once there is any forward speed. The outdoor test results (fig. 15) showed a definite increase in the standard deviation at the bottom of the engine, but this spatial variation disappears with forward speed.

The result of these comparisons indicate that, even at the low fan speeds on the outdoor test stand, extraneous turbulent flow enters the inlet and is detected on the fan blades. This turbulent flow, which could contribute to tone-like noise (ref. 11) in the far field, is seen as an increase in the broadband level and in the harmonic levels of the engine fundamental frequency on the FBMT. As the fan speed increases, effects of the test stand and/or the ground plane are identifiable as angular nonuniformities which also offer an input to tone-like noise generation. One effect that was not significantly changed was the dominance of the six-cycle-per-revolution phenomenon caused by the internal struts. This characteristic of the engine was identifiable and was of the same magnitude with or without forward speed. The six struts appear to affect only the mean pressure variation and not the standard deviation of the pressure signal. This variation of static pressure, but not the fluctuating components, with physical location would indicate a type of spatially fixed potential flow field set up by the struts. Additional data from fluctuating pressure measurements behind the fan face will be necessary to determine the exact nature of this six-cycle variation at the fan face because of the complex nature of the fan, stators, and bypass duct.

## CONCLUSIONS

As part of a program to investigate the fan noise of a turbofan engine, tests have been conducted using a JT15D engine. To aid in understanding the mechanism of the fan noise generating process, data from pressure transducers mounted directly on the fan blades were obtained during normal operation of the engine. Conventional and enhanced-signal data reduction methods were implemented to interpret the significance

of the pressure signals and to evaluate the differences in these measurements between static ground tests and wind-tunnel tests. The following conclusions were drawn from the results of these measurements.

Fan-blade-mounted transducers indicated that during the outdoor tests turbulence from the atmosphere and from the test stand affected measurements over the fan-speed range of 6750 to 13 490 rpm. These data clearly support the objections to static testing of turbofan engines as a method of determining noise characteristics without the benefit of some kind of inflow turbulence-control device.

The effect of internal struts in the bypass duct on the surface-pressure fluctuation was investigated. The effect was significant enough to be observable either outdoors or with tunnel off or tunnel on. The potential flow interaction between these struts and the fan blades are considered to be a significant source of noise in this engine.

The effect of tunnel speed was to reduce the broadband noise and the harmonic content of the fan fundamental frequency from the levels measured statically on the fan blades. Above 10 m/s, there were no other changes in the pressure spectrum on the blades. Characteristics of individual engines (for the JT15D engine, a one-cycle-per-revolution variation and a six-cycle-per-revolution variation) were unaffected by forward speed.

Spanwise characteristics of the fan-blade pressure vary greatly and appear to be most affected by the transition of the measurement location from subsonic speed to supersonic speeds. Below supersonic tip speeds, engine characteristics (i.e., the six-cycle variation per revolution) dominate the signal. At supersonic tip speeds, no single characteristic is identifiable.

Langley Research Center
National Aeronautics and Space Administration
Hampton, VA 23665
February 19, 1982

REFERENCES


1. Feiler, Charles E.; and Groeneweg, John F.: Summary of Forward Velocity Effects on Fan Noise. NASA TM-73722, 1977.

2. Povinelli, Frederick P.; and Dittmar, James H.: Installation Caused Flow Distortion and Its Effect on Noise From a Fan Designed for Turbofan Engines. NASA TM X-68105, 1972.

3. Hanson, Donald B.: The Spectrum of Turbomachine Rotor Noise Caused by Inlet Guide Vane Wakes and Atmospheric Turbulence. HSER 6191, Hamilton Standard Div., United Aircraft Corp., May 14, 1973.

4. Hanson, Donald B.: Study of Noise Sources in a Subsonic Fan Using Measured Blade Pressures and Acoustic Theory. NASA CR-2574, 1975.

5. Rogers, D. F.; and Ganz, U. W.: Aerodynamic Assessment of Methods To Simulate Flight Inflow Characteristics During Static Testing. AIAA-80-1023, June 1980.

6. Ganz, Ulrich W.: Analytical Investigation of Fan Tone Noise Due to Ingested Atmospheric Turbulence. NASA CR-3302, 1980.

7. Jones, W. L.; McArdle, J. G.; and Homyak, L.: Evaluation of Two Inflow Control Devices for Flight Simulation of Fan Noise Using a JT15D Engine. AIAA Paper 79-0654, Mar. 1979.

8. Heidmann, M. F.; Saule, A. V.; and McArdle, J. G.: Analysis of Radiation Patterns of Interaction Tones Generated by Inlet Rods in the JT15D Engine. AIAA Paper 79-0581, Mar. 1979.

9. McArdle, J. G.; Jones, W. L.; Heidelberg, L. J.; and Homyak, L.: Comparison of Several Inflow Control Devices for Flight Simulation of Fan Tone Noise Using a JT15D-1 Engine. NASA TM-81505, 1980.

10. Preisser, J. S.; Schoenster, J. A.; Golub, R. A.; and Horne, C.: Unsteady Fan Blade Pressure and Acoustic Radiation From a JT15D-1 Turbofan Engine at Simulated Forward Speed. AIAA-81-0096, Jan. 1981.

11. Englund, David R.; Grant, Howard P.; and Lanati, George A.: Measuring Unsteady Pressure on Rotating Compressor Blades. NASA TM-79159, [1979].

12. Knight, Vernie H., Jr.: In-Flight Jet Engine Noise Measurement System. Paper presented at the ISA 27th International Instrumentation Symposium (Indianapolis, Indiana), Apr. 27-30, 1981.

13. Hanson, Donald B.: Spectrum of Rotor Noise Caused by Atmospheric Turbulence. J. Acoust. Soc. America, vol. 56, no. 1, July 1974, pp. 110-126.

14. Hodder, Brent K.: An Investigation of Possible Causes for the Reduction of Fan Noise in Flight. AIAA Paper No. 76-585, July 1976.

15. Tyler, J. M.; and Sofrin, T. G.: Axial Flow Compressor Noise Studies. SAE Trans., vol. 70, 1962, pp. 309-332.

TABLE I.- JT15D SPECIFICATIONS

| | |
|---|---|
| Fan speed (max.), rpm | 16 000 |
| Fan pressure ratio | 1.5 |
| Bypass ratio (max.) | 3.3 |
| Rotor blades | 28 |
| Rotor diameter, m | 0.533 |
| Hub/tip ratio | 0.405 |
| Bypass-stator vanes | 66 |
| Core-stator vanes | [a]71 |
| Rotor/bypass-stator spacing | 1.83 |
| Rotor/core-stator spacing | [b]0.63 |
| Compressor speed (max.), rpm | 32 760 |
| Core exhaust area, $m^2$ | 0.051 |
| Bypass exhaust area, $m^2$ | 0.092 |

[a]Production engine has 33 core-stator vanes.

[b]Production engine core-stator spacing is 0.28, normalized to fan-blade root chord.

TABLE II.- STABILITY OF FAN SPEED OF JT15D ENGINE IN WIND TUNNEL

| Configuration[a] (Tunnel speed, m/s) | Fan speed, rpm | | | |
|---|---|---|---|---|
| | Nominal | Minimum | Maximum | Variation |
| EMT | 12 000 | 11 931 | 11 979 | 48 |
| (<6) | 10 500 | 10 481 | 10 520 | 39 |
| EMT | 12 000 | 11 960 | 11 979 | 19 |
| (10) | 10 500 | 10 491 | 10 510 | 19 |
| EMT | 12 000 | 11 950 | 11 979 | 29 |
| (31) | 10 500 | 10 529 | 10 548 | 19 |
| EMT | 12 000 | 11 969 | 11 979 | 10 |
| (44) | 10 500 | | 10 510 | 0 |
| ET | 12 000 | 12 046 | 12 113 | 67 |
| (<6) | | | | |
| ET | 12 000 | | 12 008 | 0 |
| (31) | 10 500 | 10 481 | 10 491 | 10 |
| ET | 12 000 | 11 988 | 11 998 | 10 |
| (57) | 10 500 | 10 472 | 10 491 | 19 |

[a]Components: E - engine, M - muffler, T - traverse rail.

TABLE III.- EFFECT OF FORWARD SPEED ON FBMT RESPONSE AT FUNDAMENTAL FAN FREQUENCY AND AT SIXTH HARMONIC FREQUENCY (10 500 rpm)

| Tunnel speed, m/s (Configuration[a]) | Sound pressure level, dB, at - (Enhanced sound pressure level, dB) | | | | | |
|---|---|---|---|---|---|---|
| | FBMT G | | FBMT H | | FBMT I | |
| | Fundamental | 6th harmonic | Fundamental | 6th harmonic | Fundamental | 6th harmonic |
| <6 (EMT) | 138 (137) | 139 (138) | 139 (139) | 140 (140) | 143 (142) | 140 (139) |
| 10 (EMT) | 138 (136) | 139 (137) | 139 (139) | 140 (140) | 140 (140) | 140 (139) |
| 31 (EMT) | 138 (137) | 138 (137) | 139 (138) | 141 (140) | 140 (140) | 139 (139) |
| 44 (EMT) | 138 (137) | 137 (137) | 139 (139) | 140 (140) | 139 (139) | 139 (139) |
| 31 (ET) | 137 (135) | 139 (137) | 139 (139) | 141 (140) | 139 (139) | 140 (139) |
| 57 (ET) | 137 (136) | 138 (137) | 139 (139) | 141 (140) | 139 (139) | 139 (138) |

[a]Components: E - engine, M - muffler, T - traverse rail.

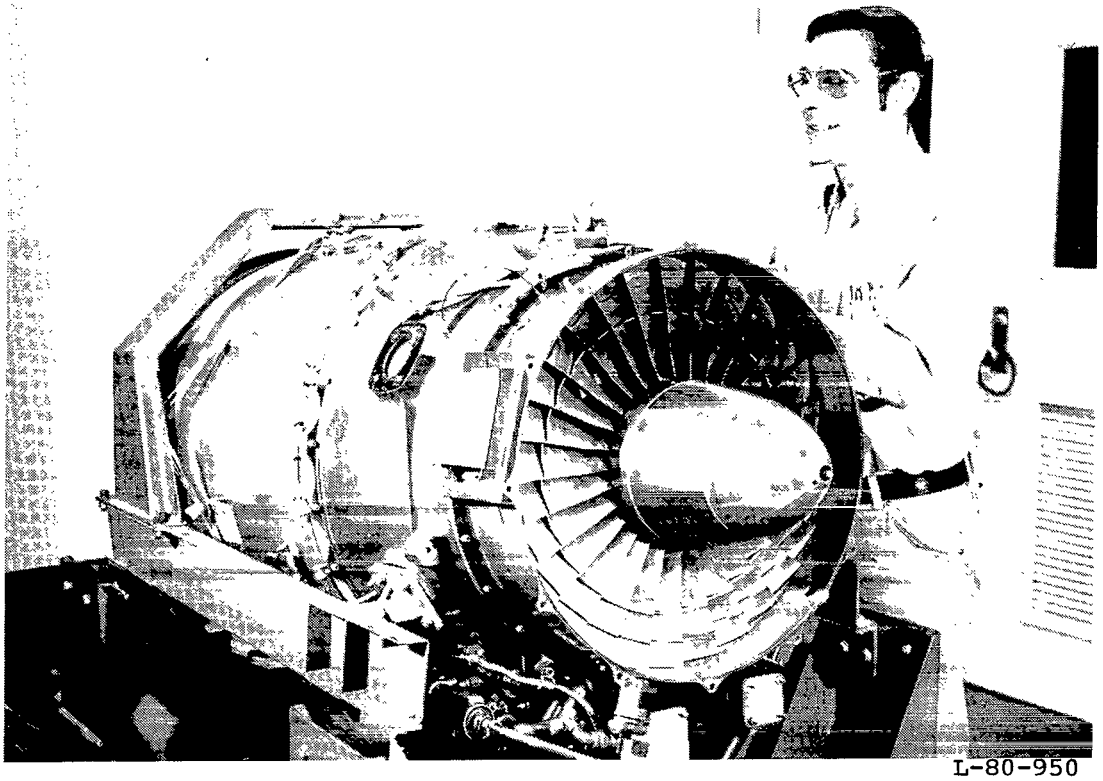


Figure 1.- JT15D engine (nacelle and inlet removed).

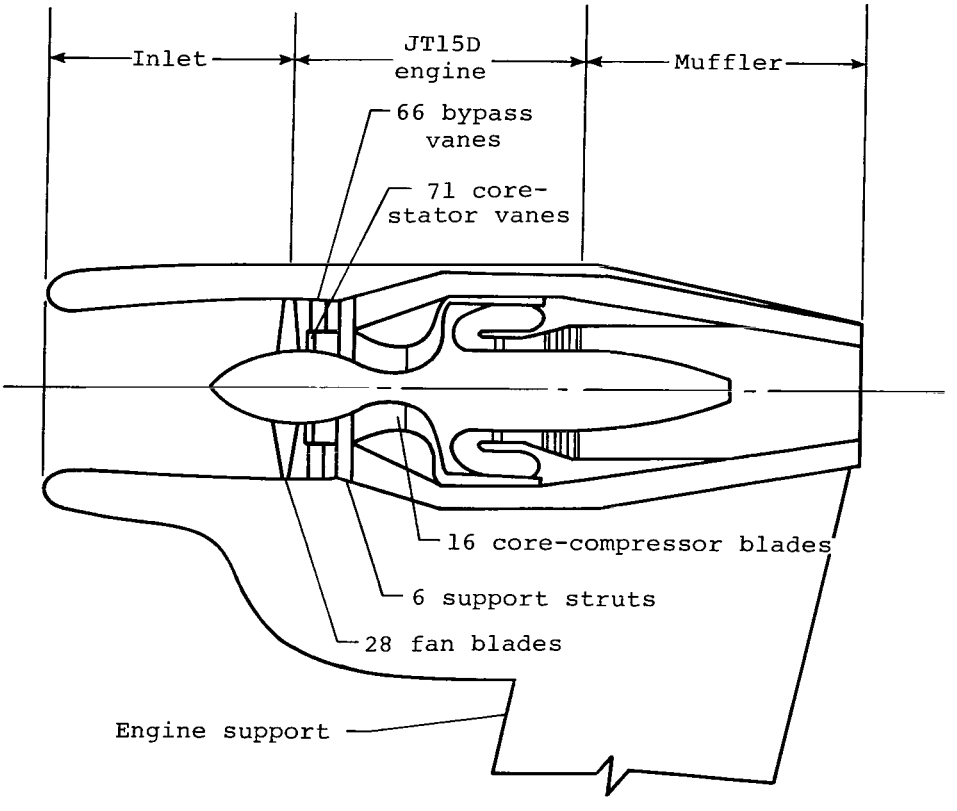


Figure 2.- Cross-section sketch of JT15D engine in test configuration.

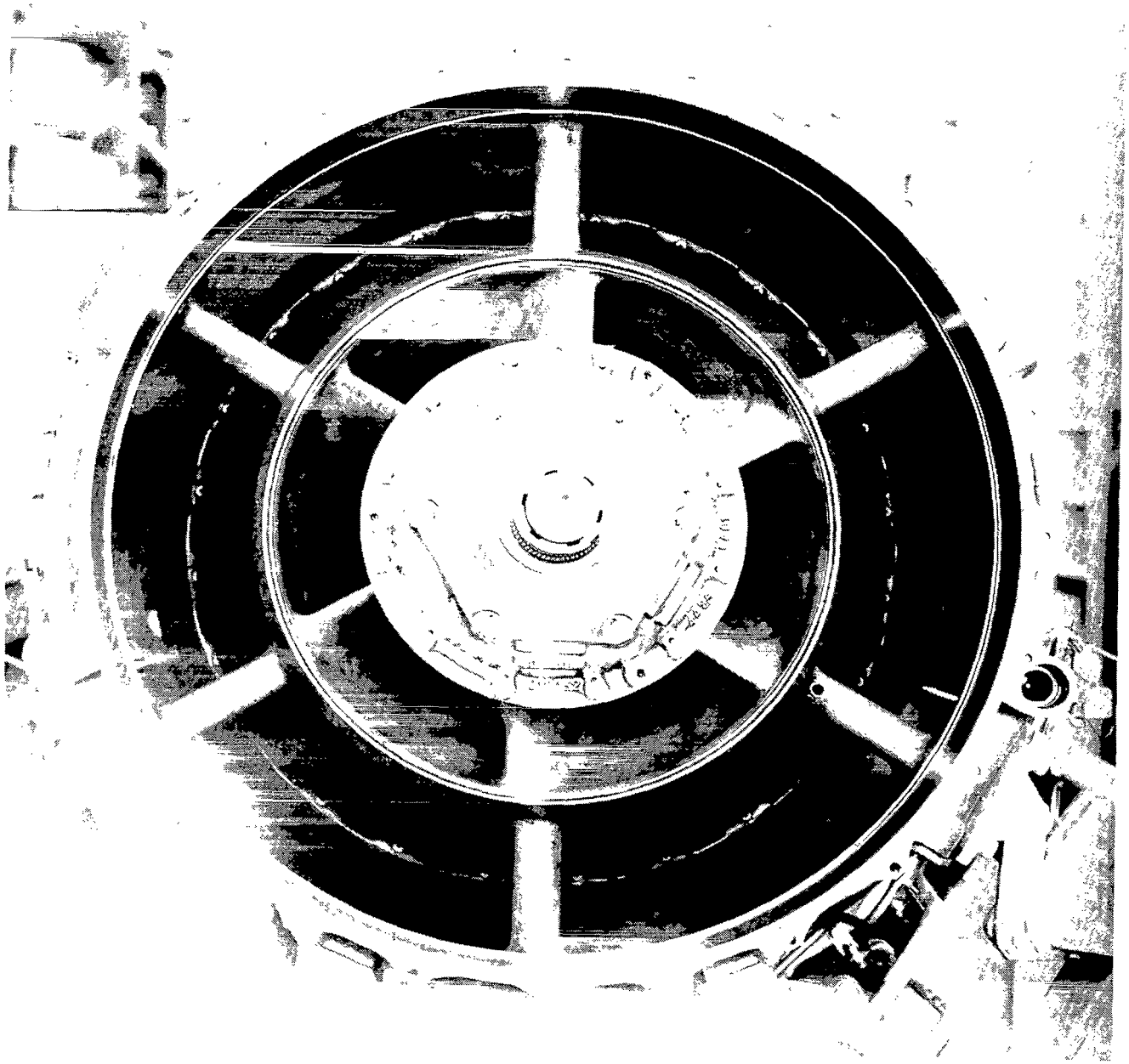

L-80-4221

Figure 3.- Internal structure of JT15D engine showing six support struts in bypass duct.

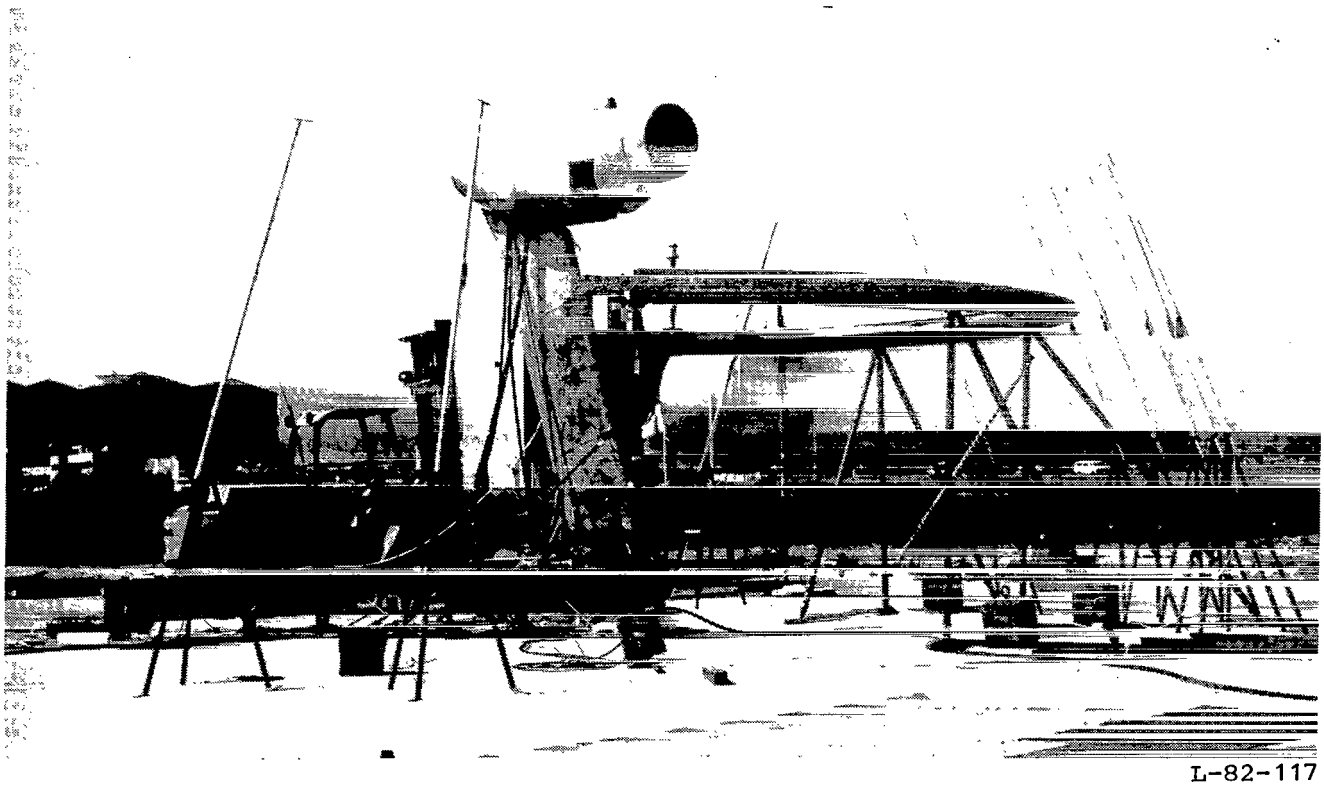

L-82-117

Figure 4.- JT15D engine on outdoor static-test stand at Ames Research Center.

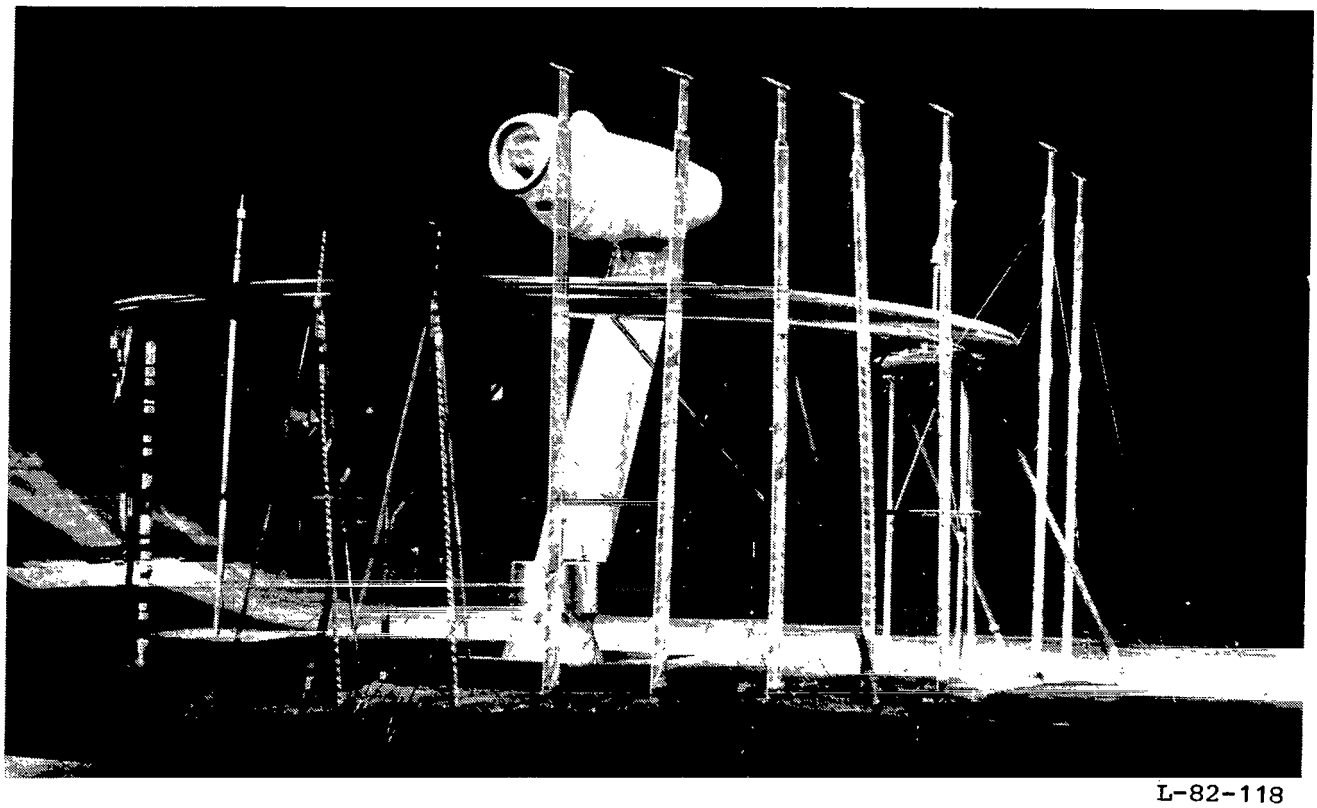

L-82-118

Figure 5.- JT15D engine mounted in Ames 40- by 80-Foot Wind Tunnel.

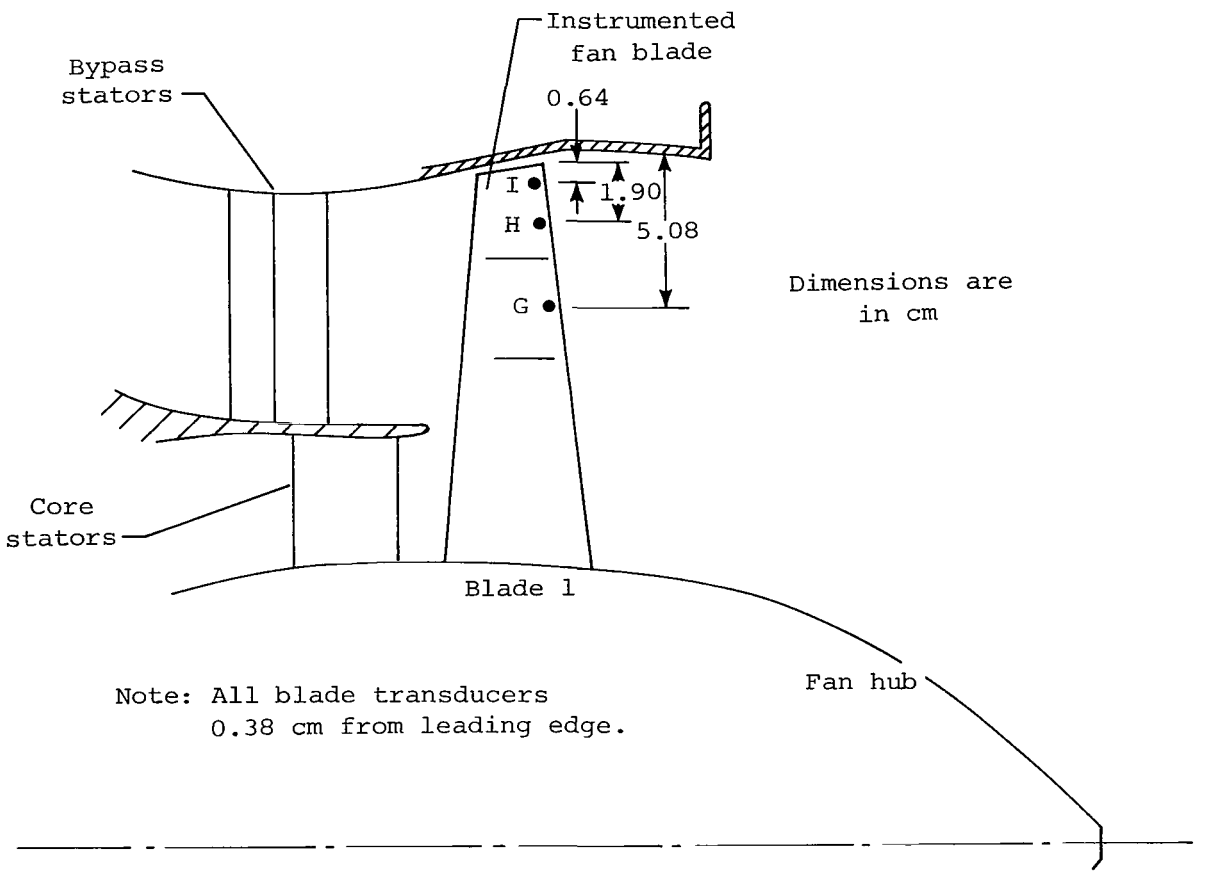


Figure 6.- Schematic showing locations of fan-blade-mounted transducers.

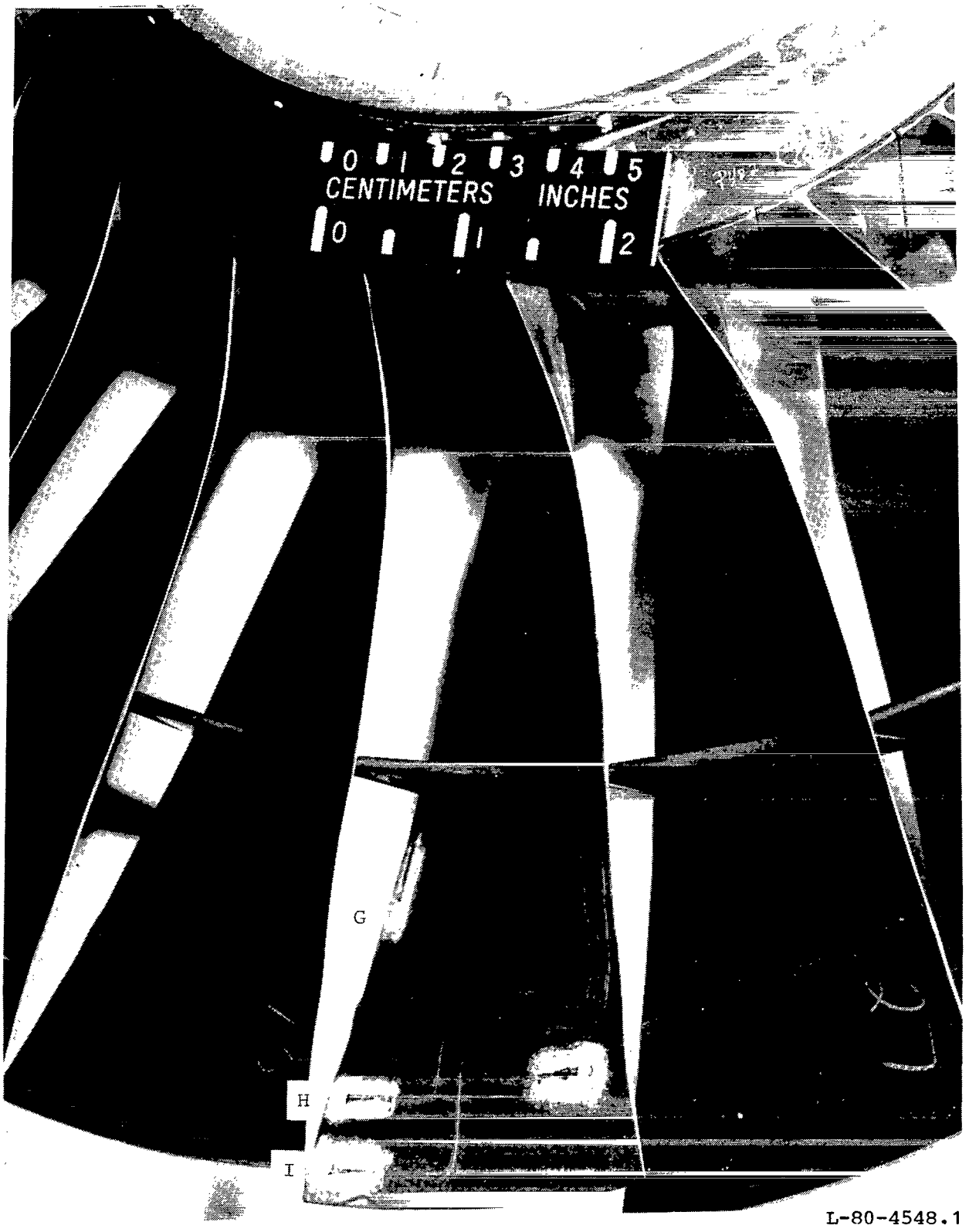


Figure 7.- Fan-blade-mounted transducers used in this study.

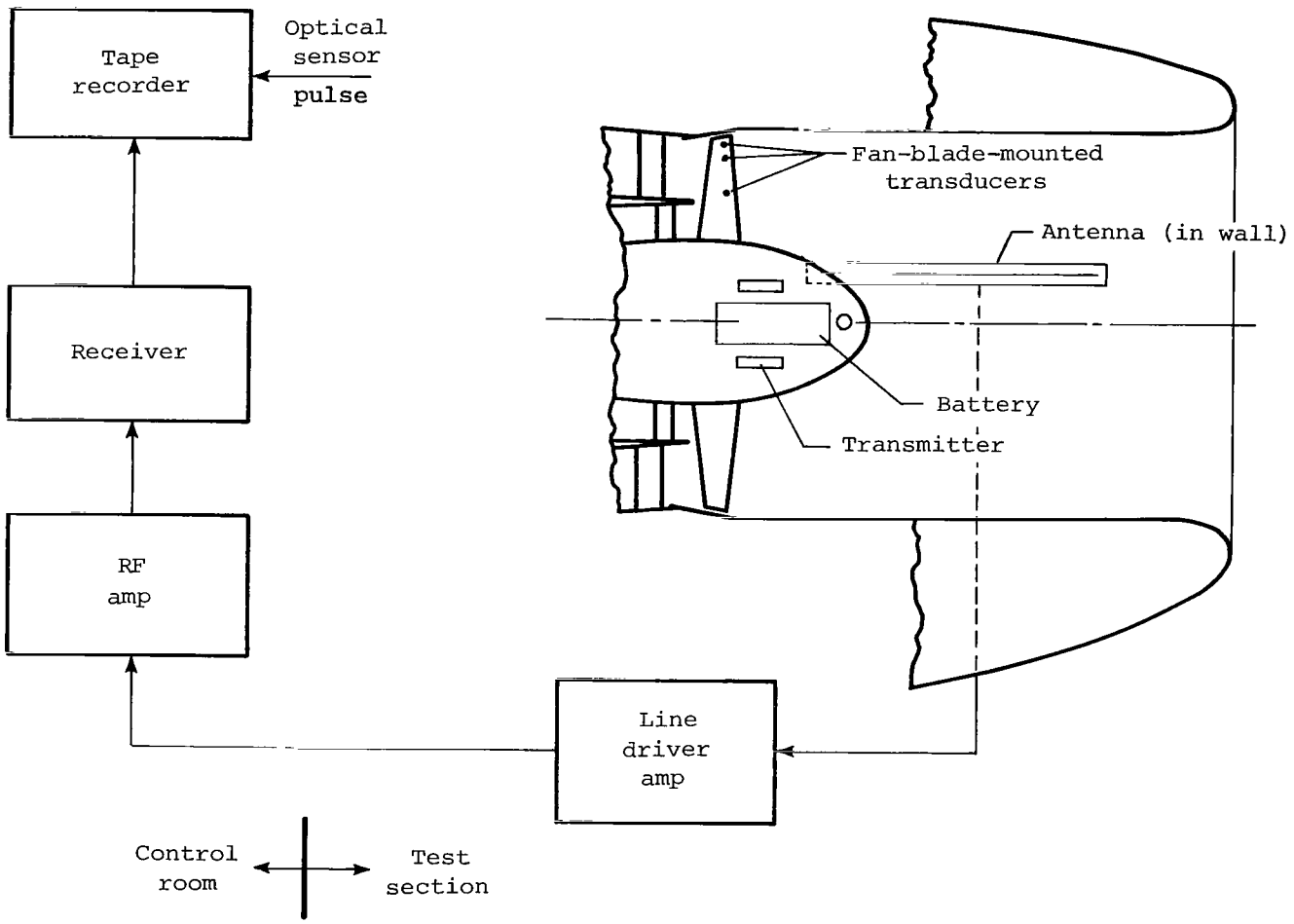


Figure 8.- Sketch of fan-blade-mounted-transducer data system in JT15D engine.

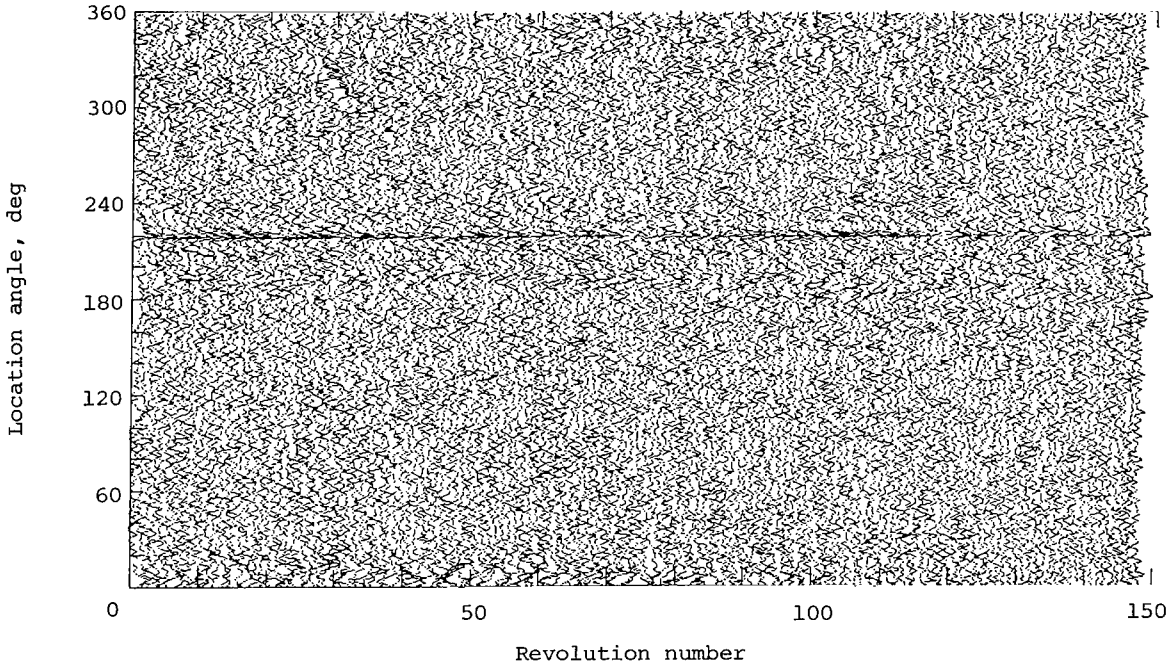


(a) Space/time history.

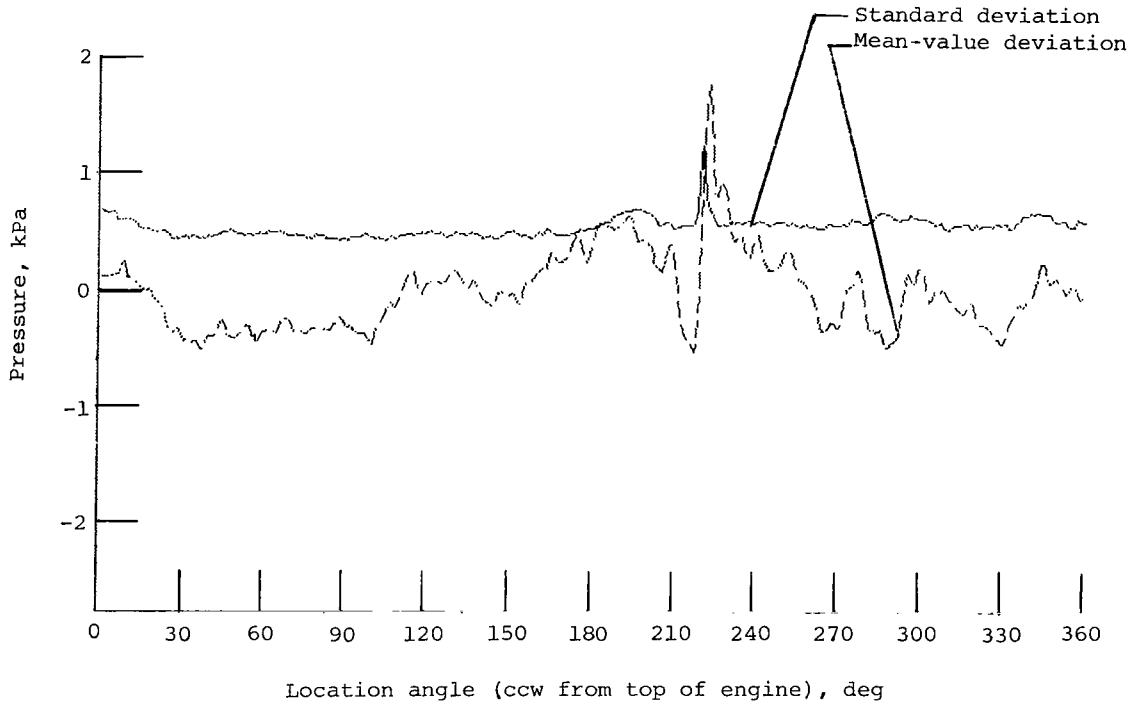


(b) Standard deviation and mean value.

Figure 9.- Data analysis results for fan-blade-mounted transducer H with calibration rod in place; 6710 rpm.

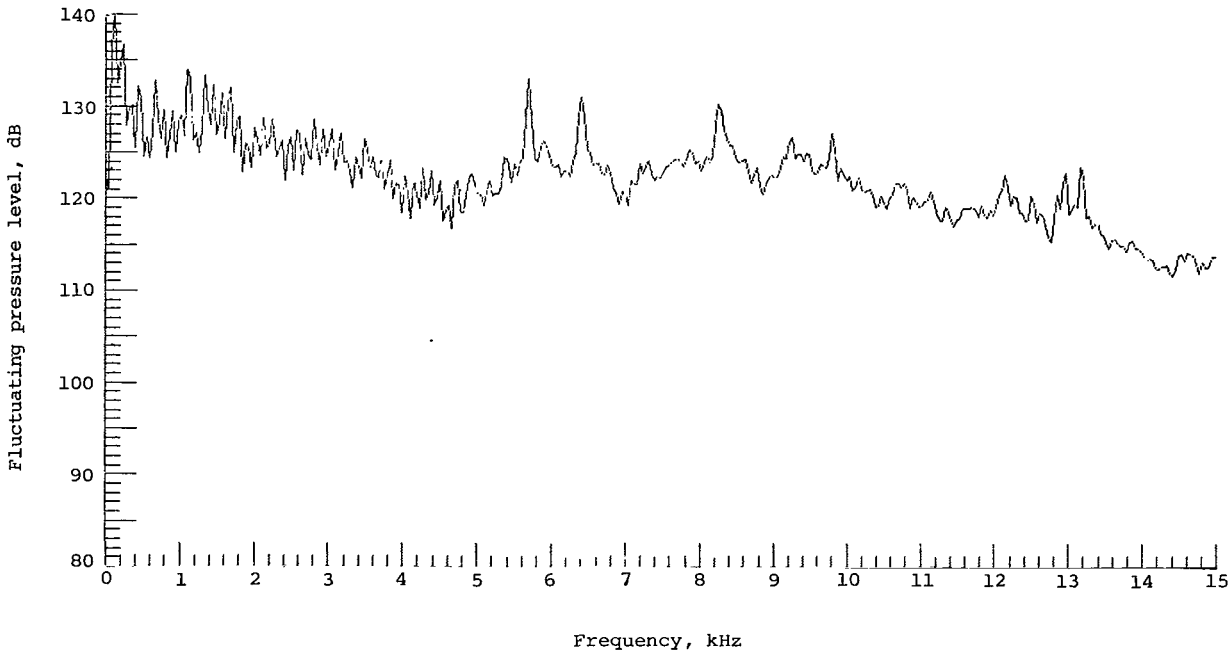


(c) Overall spectral analysis.

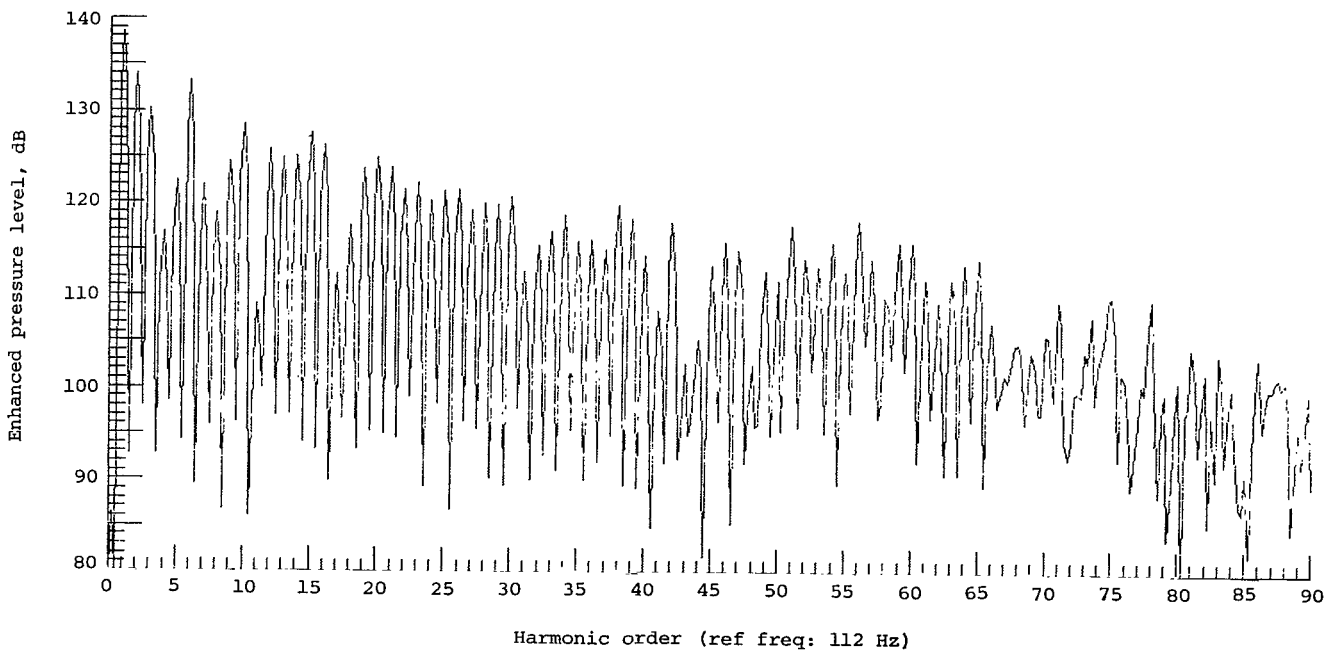


(d) Enhanced-signal spectral analysis.

Figure 9.- Concluded.

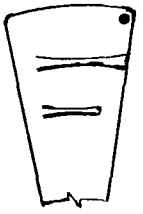

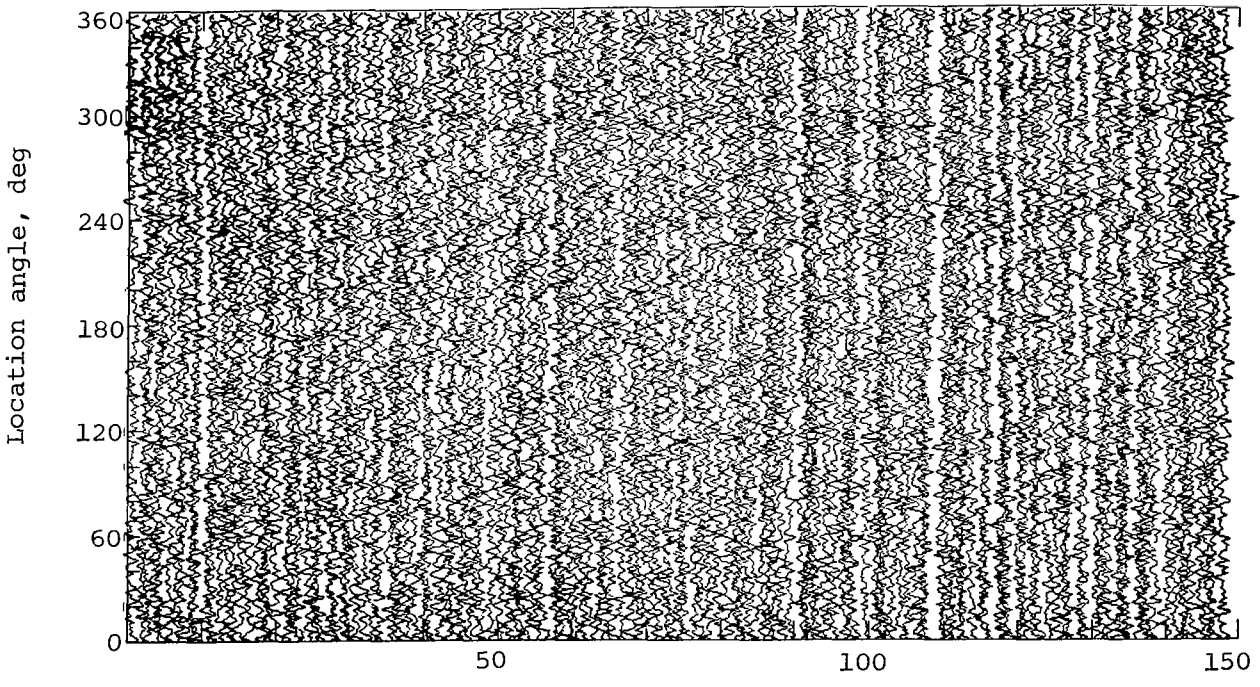


(a) FBMT I.

Figure 10.- Space/time history for fan-blade-mounted transducers; outdoor test stand, 6750 rpm.

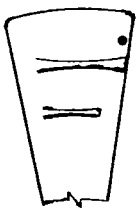

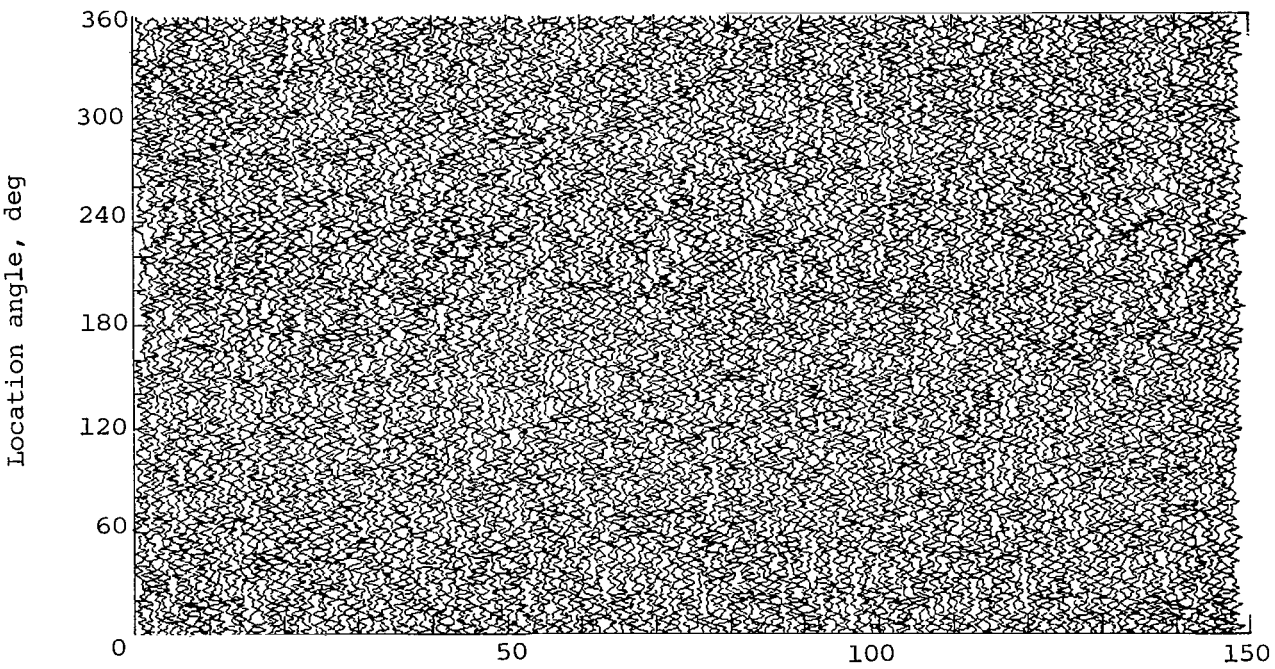


(b) FBMT H.

Figure 10.- Continued.

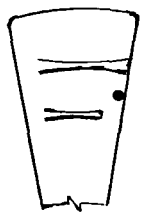


(c) FBMT G.

Figure 10.- Concluded.

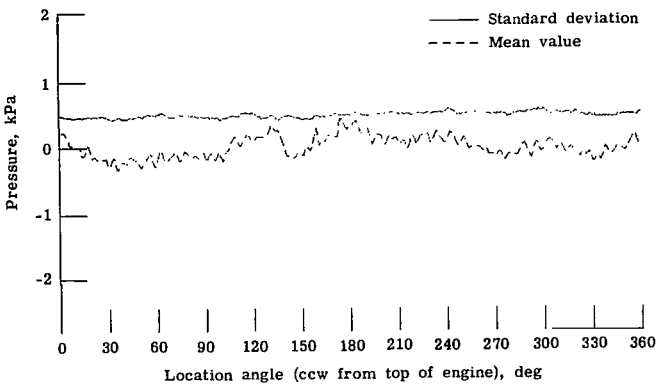


(a) FBMT I.

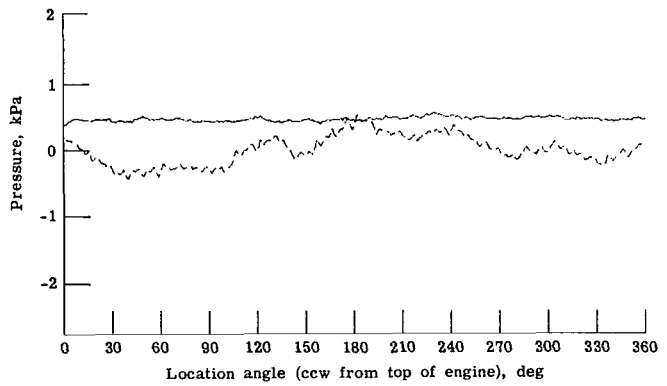


(b) FBMT H.

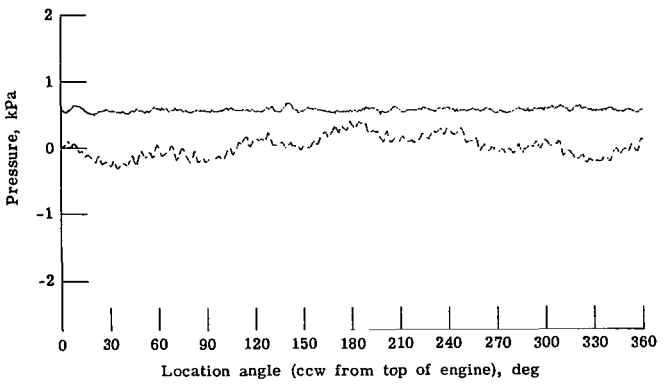


(c) FBMT G.

Figure 11.- Standard-deviation and mean-value plots for fan-blade-mounted transducers; outdoor test stand, 6750 rpm.

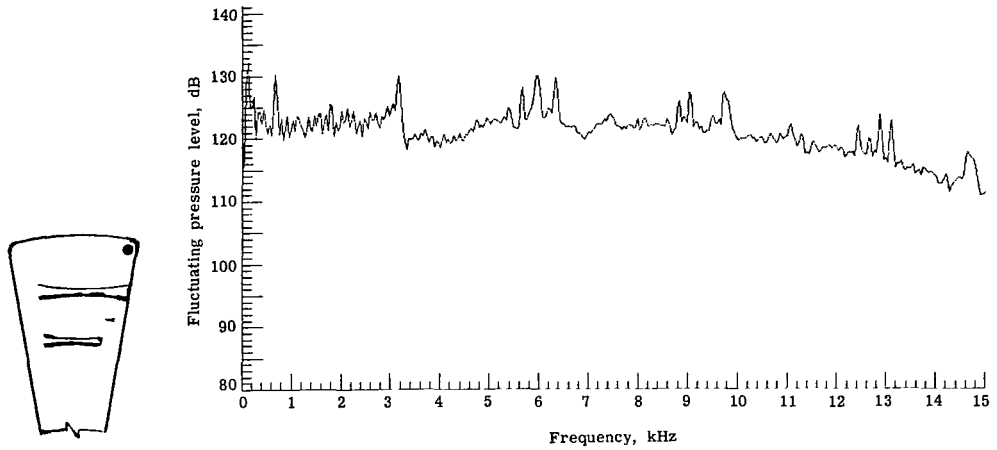


(a) FBMT I.

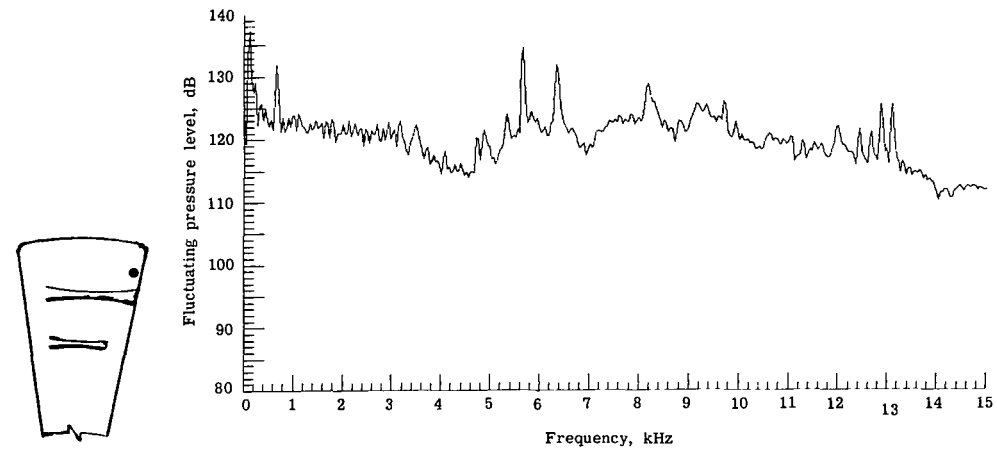


(b) FBMT H.

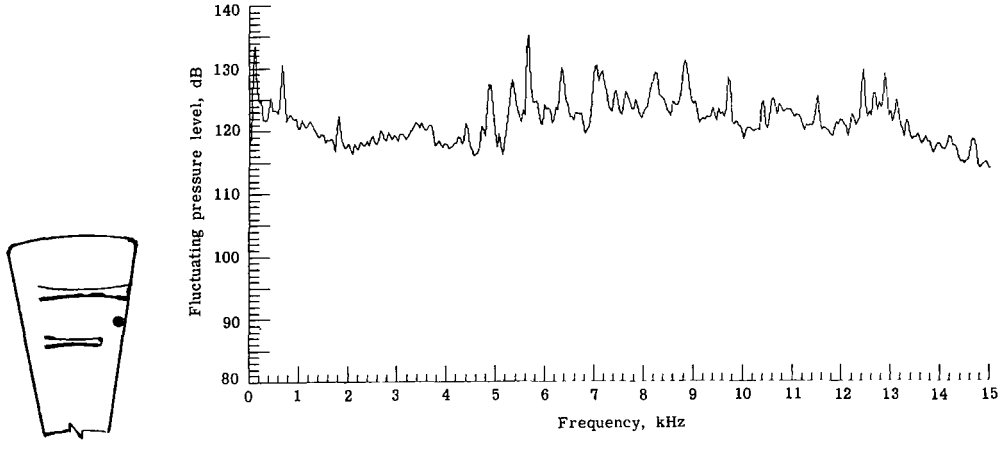


(c) FBMT G.

Figure 12.- Overall spectral plots for fan-blade-mounted transducers; outdoor test stand, 6750 rpm.

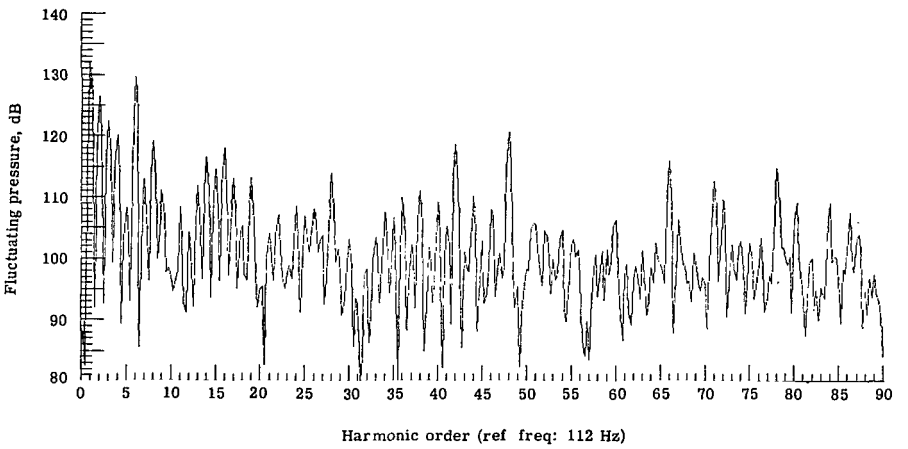


(a) FBMT I.

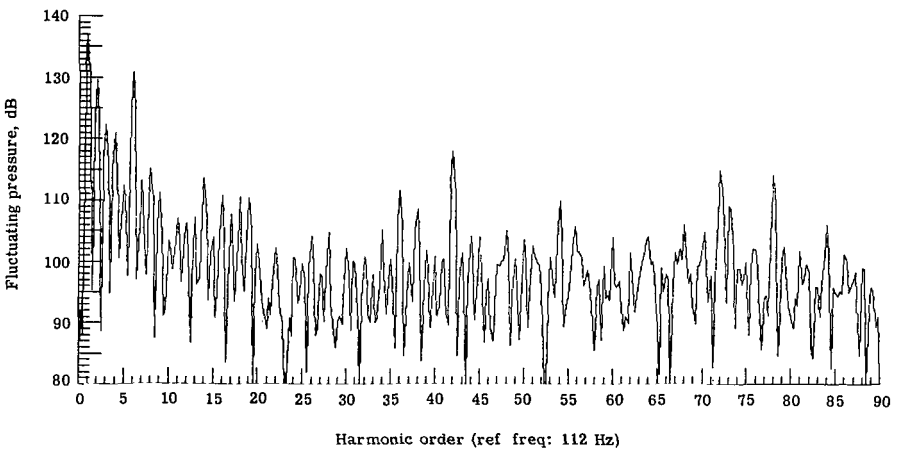


(b) FBMT H.

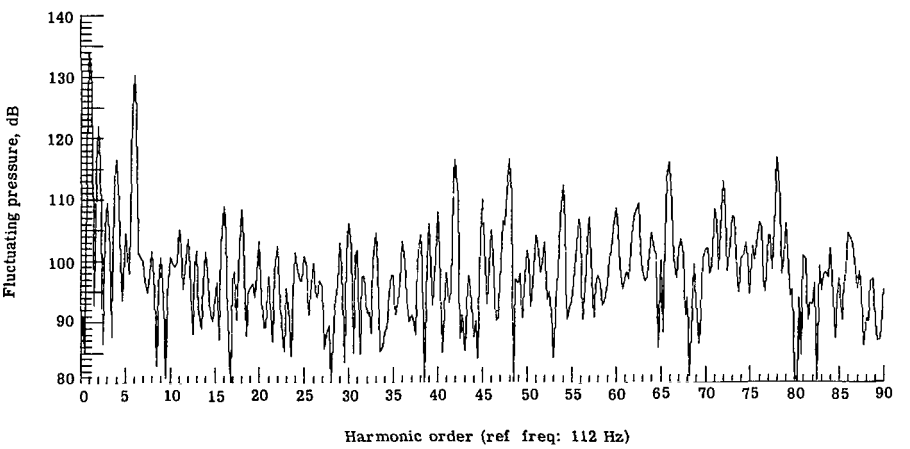


(c) FBMT G.

Figure 13.- Enhanced-signal spectral plots for fan-blade-mounted transducers; outdoor test stand, 6750 rpm.

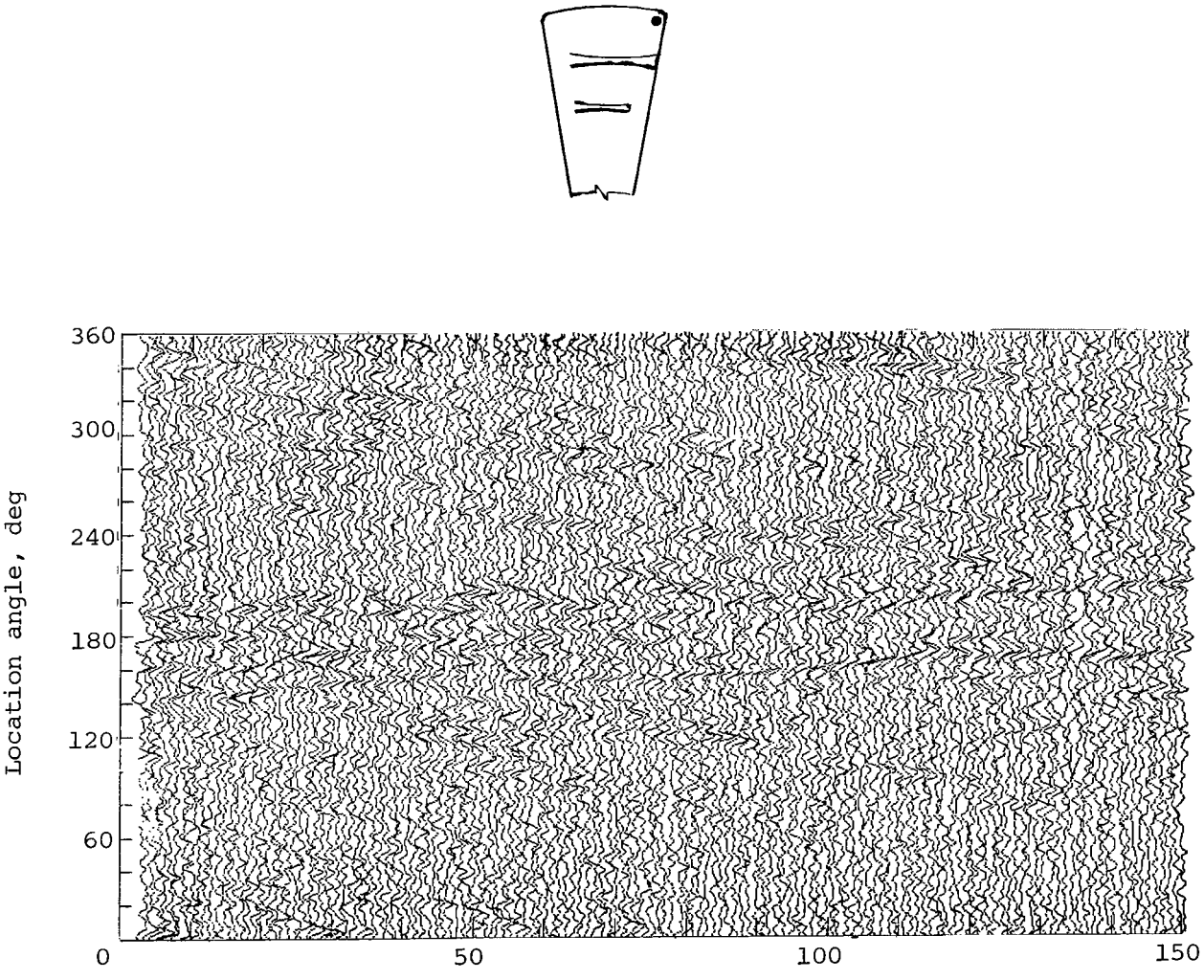


(a) FBMT I.

Figure 14.- Space/time-history plots for fan-blade-mounted transducers; outdoor test stand, 13 490 rpm.

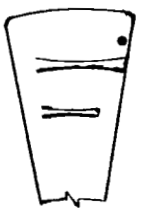

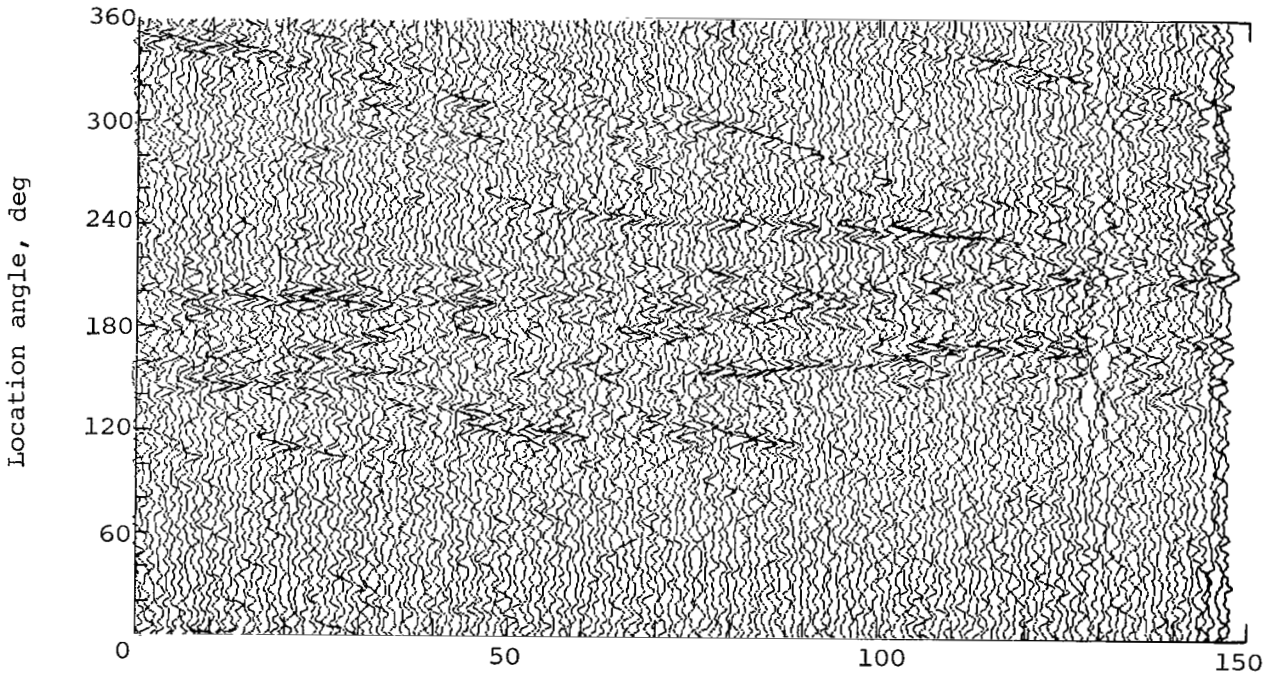


(b) FBMT H.

Figure 14.- Continued.

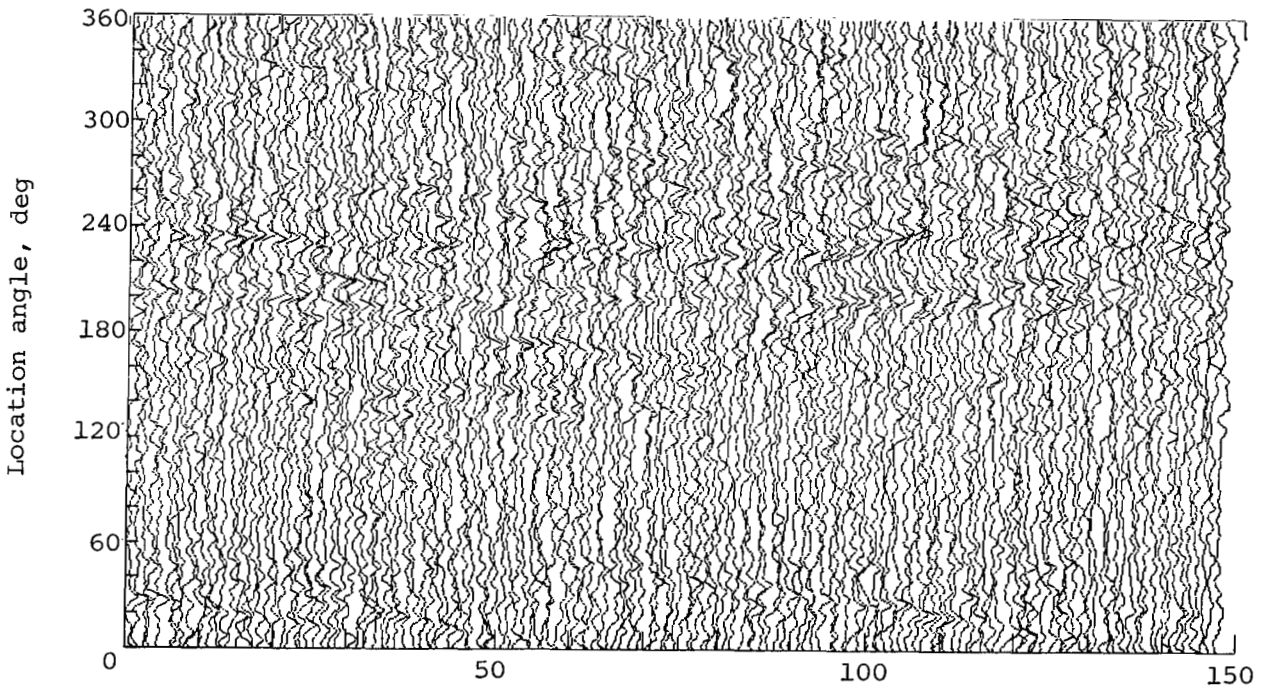


(c) FBMT G.

Figure 14.- Concluded.


(a) FBMT I.

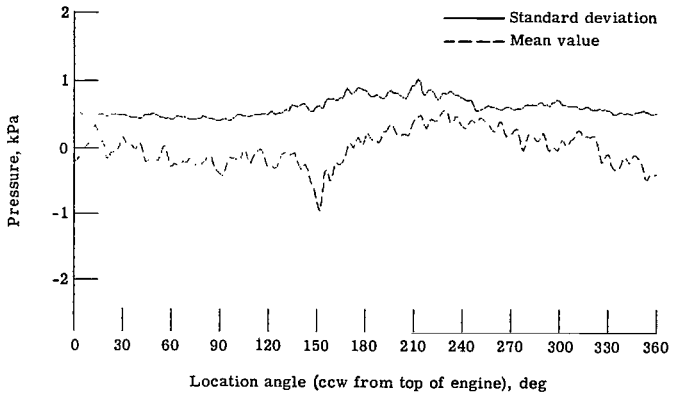


(b) FBMT H.

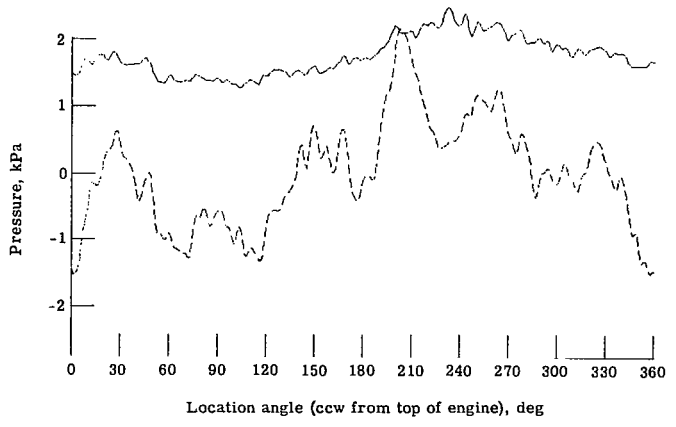


(c) FBMT G.

Figure 15.- Standard-deviation and mean-value plots for fan-blade-mounted transducers; outdoor test stand, 13 490 rpm.

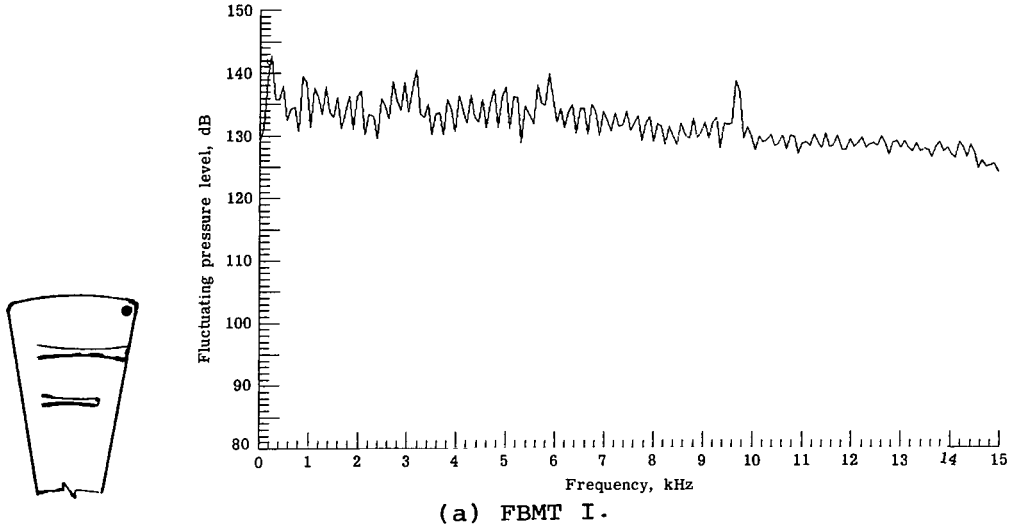


(a) FBMT I.

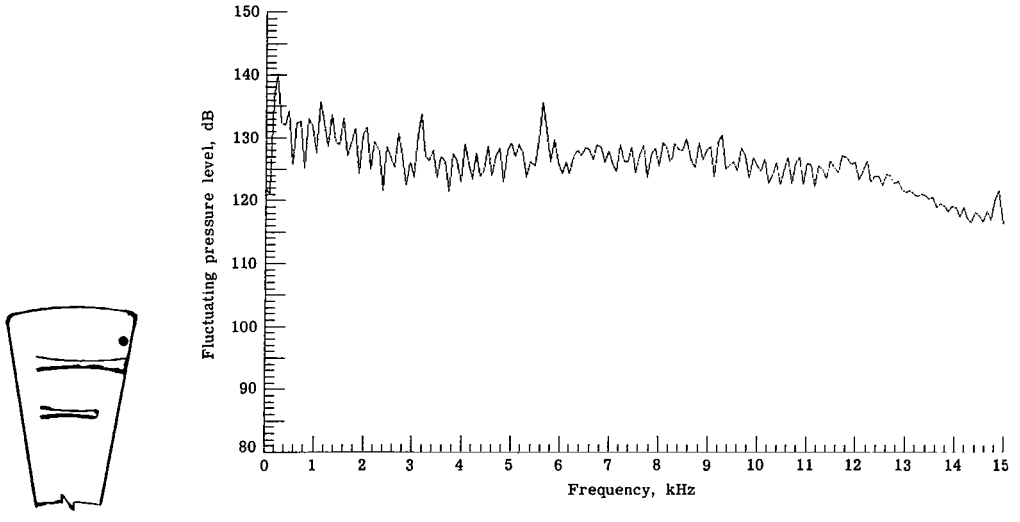


(b) FBMT H.

Figure 16.- Overall spectral plots for fan-blade-mounted transducers; outdoor test stand, 13 490 rpm.

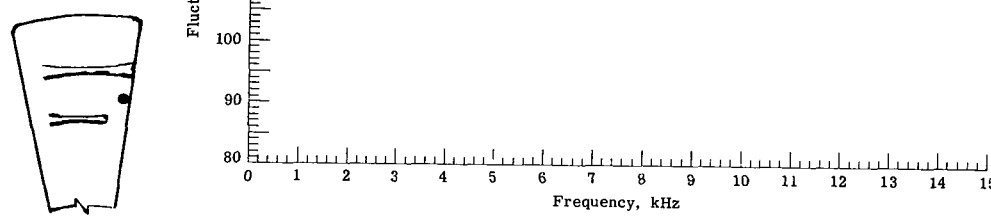


(c) FBMT G.

Figure 16.- Concluded.

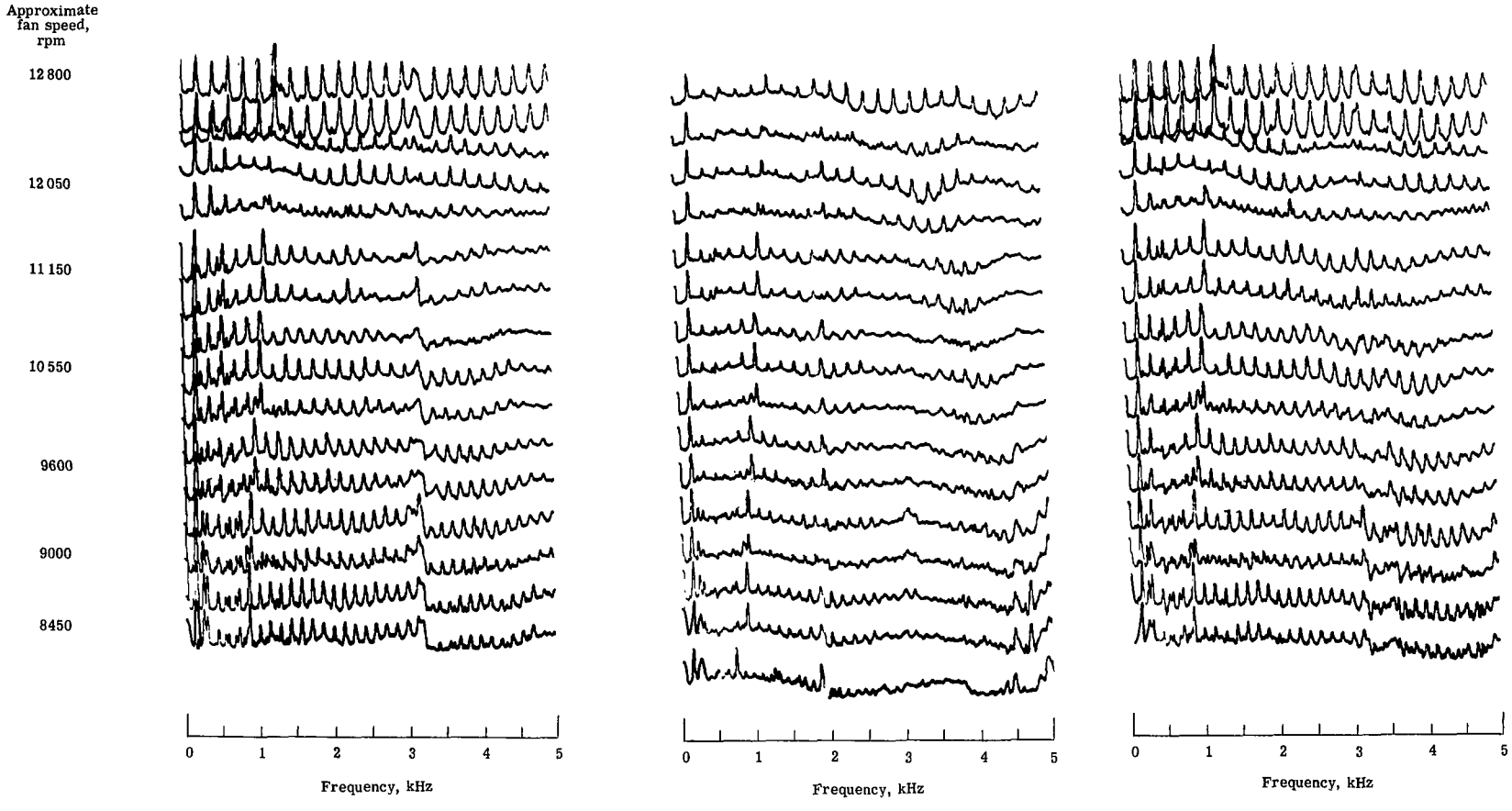


Figure 17.- Spectral plots for fan-blade-mounted-transducer data from sweep of engine speed; tunnel off, Bandwidth of analysis = 10 Hz.

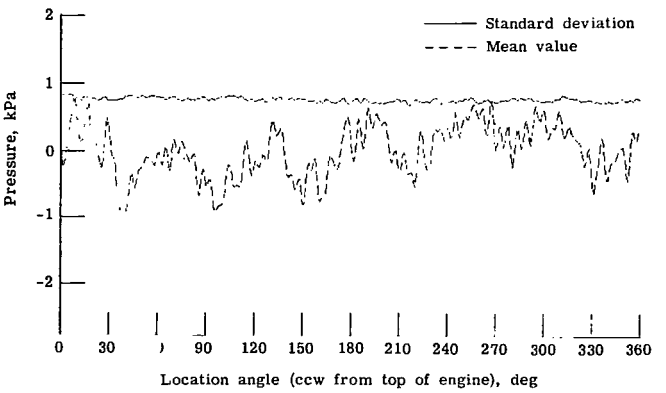


(a) FBMT I.

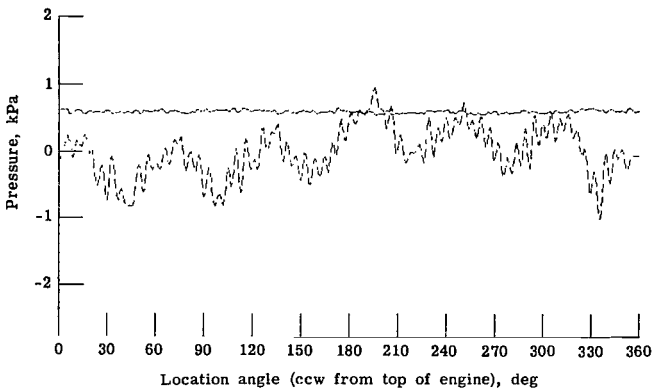


(b) FBMT H.

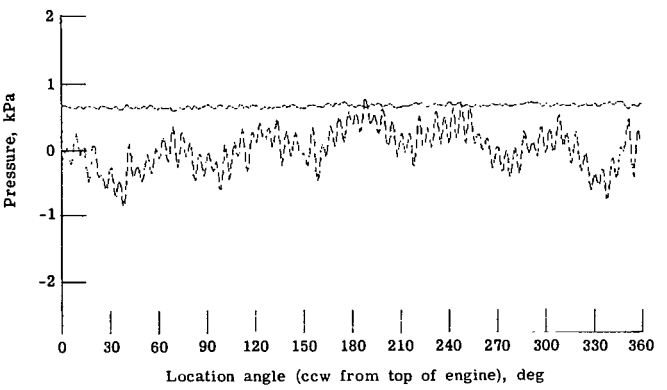


(c) FBMT G.

Figure 18.- Standard-deviation and mean-value plots for fan-blade-mounted transducers; 10 500 rpm, 44 m/s tunnel speed.

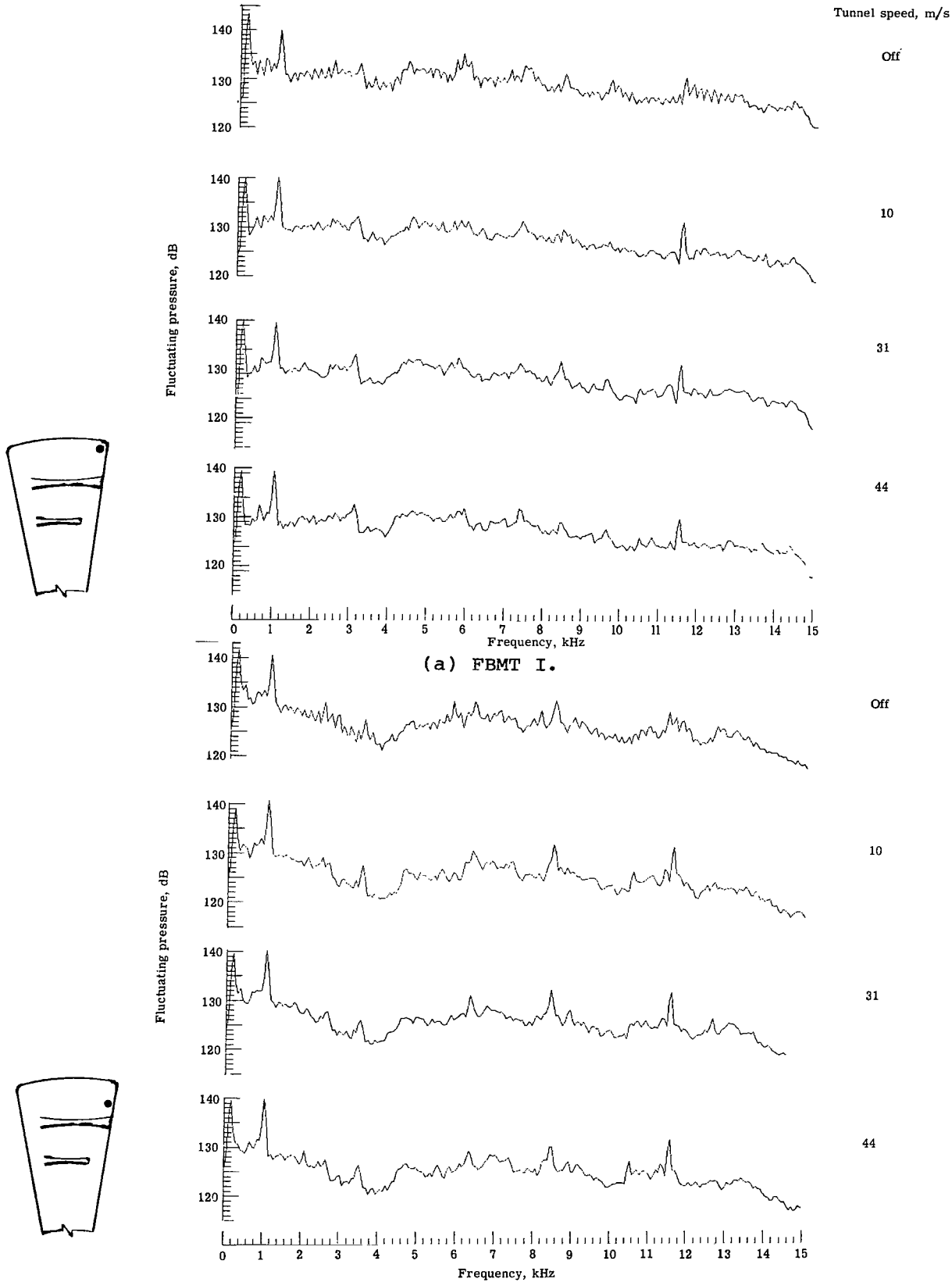


Figure 19.- Overall spectral plots for fan-blade-mounted transducers; 10 500 rpm.

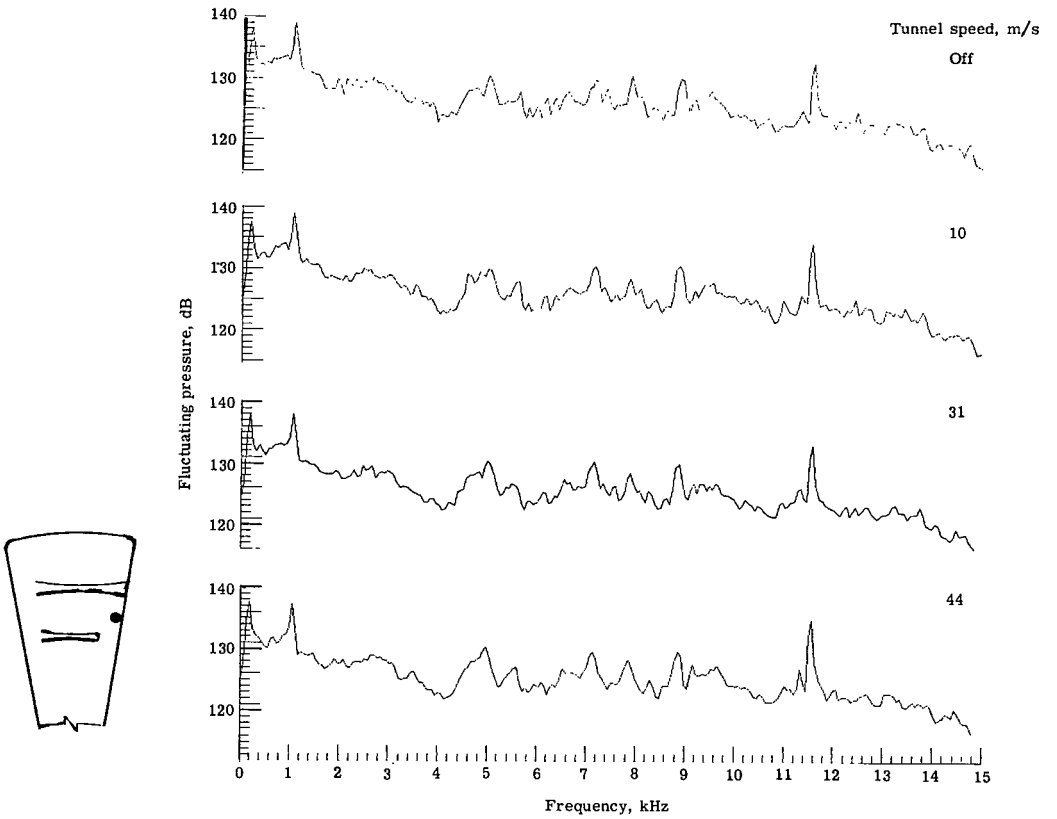


(c) FBMT G.

Figure 19.- Concluded.

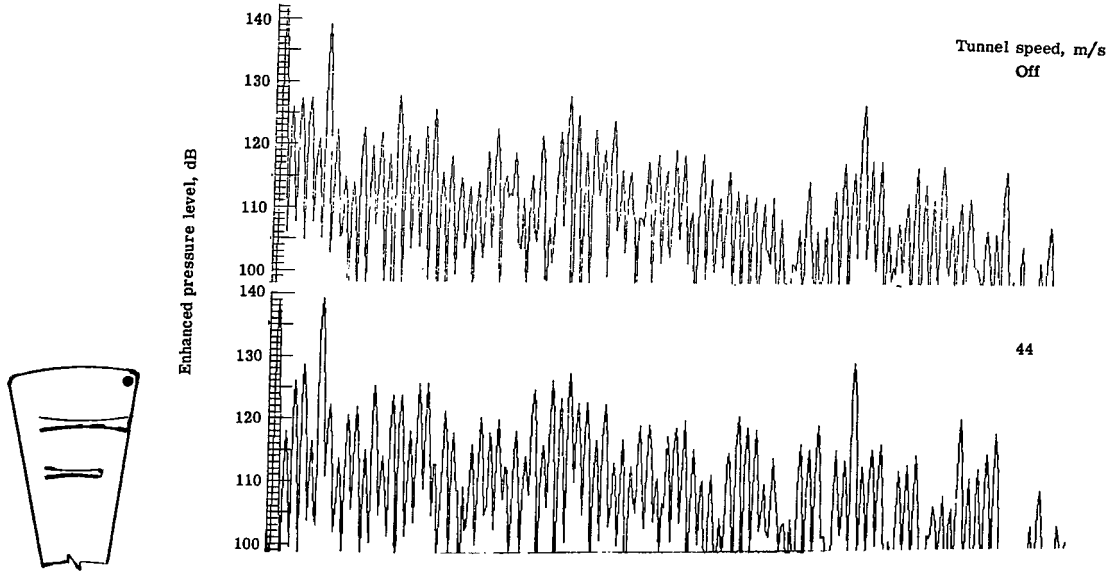


(a) FBMT I.

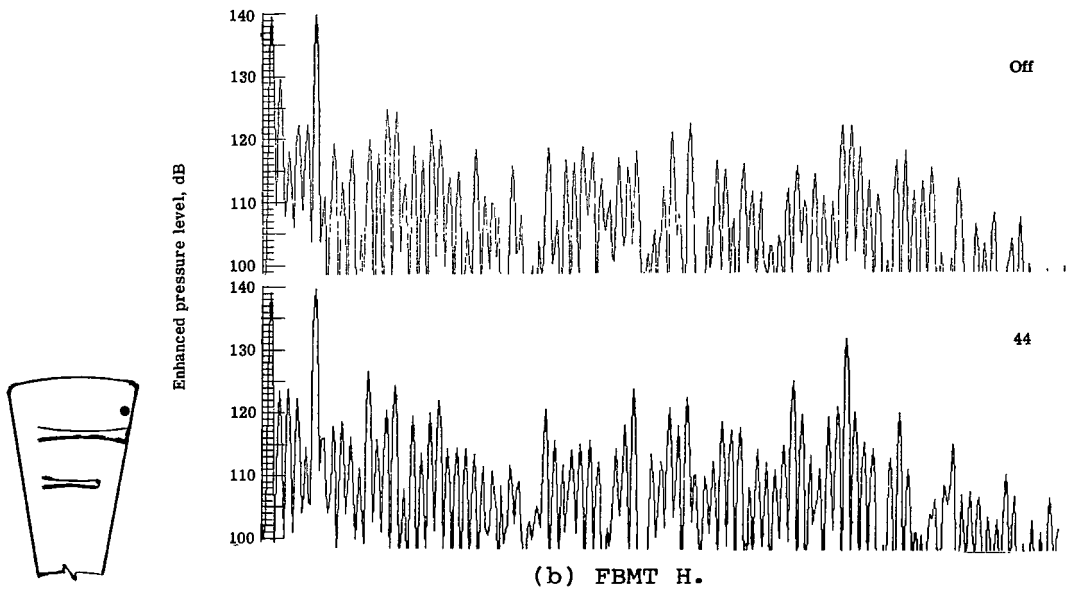


(b) FBMT H.

Figure 20.- Enhanced-signal spectral plots for fan-blade-mounted transducers; 10 500 rpm.

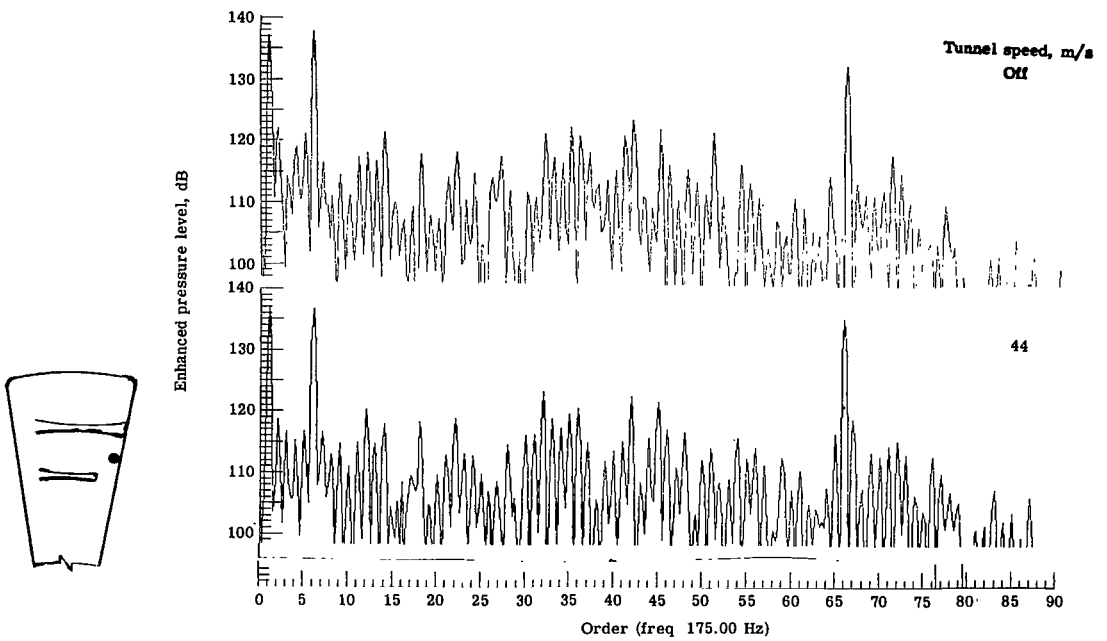


(c) FBMT G.

Figure 20.- Concluded.

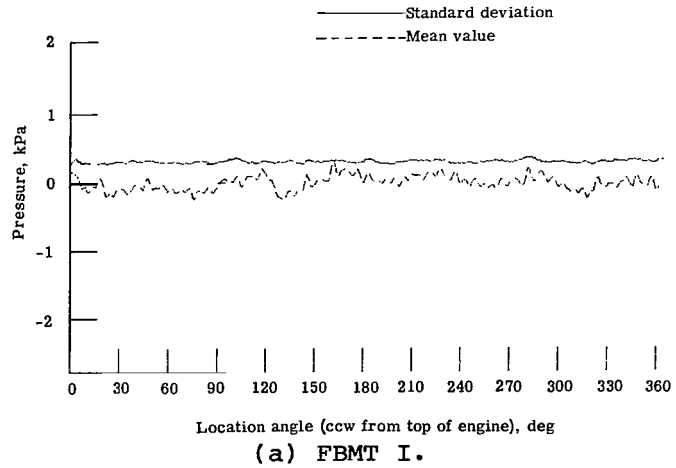


(a) FBMT I.

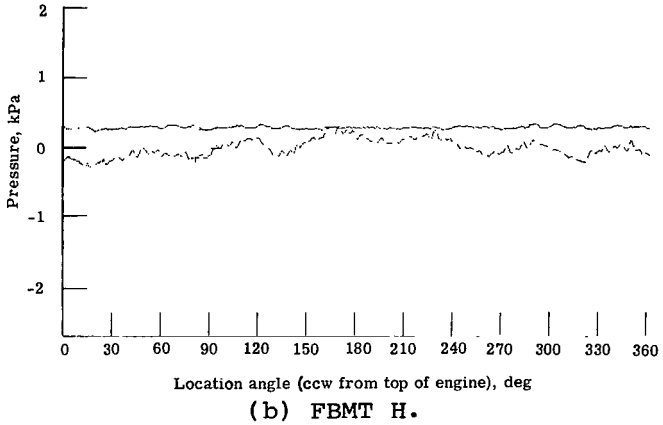


(b) FBMT H.

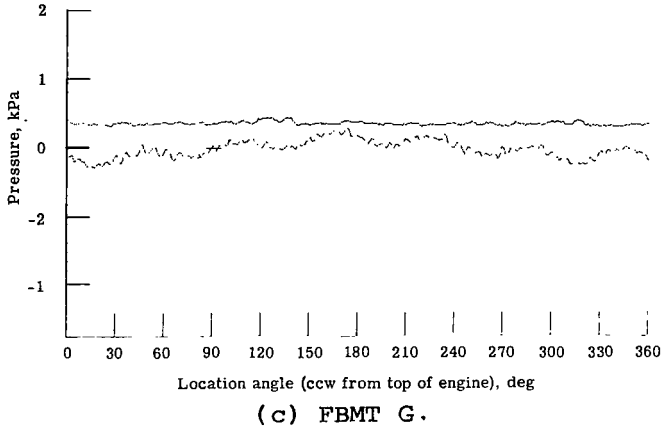


(c) FBMT G.

Figure 21.- Standard-deviation and mean-value plots for fan-blade-mounted transducers; 6750 rpm, 44 m/s tunnel speed.

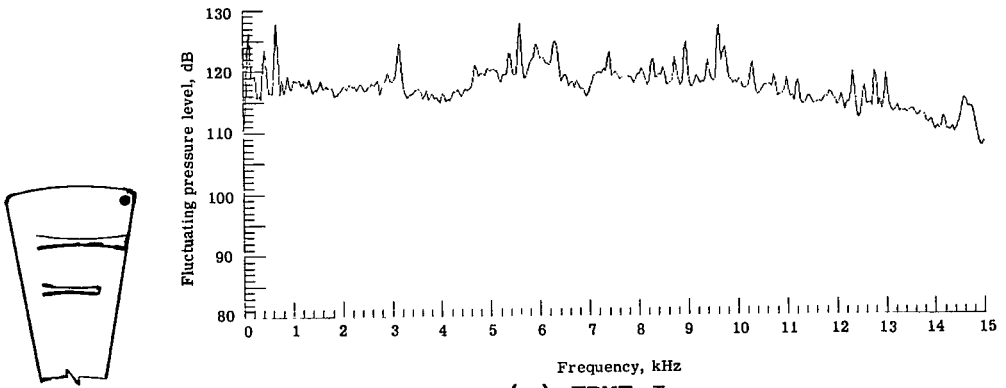


(a) FBMT I.

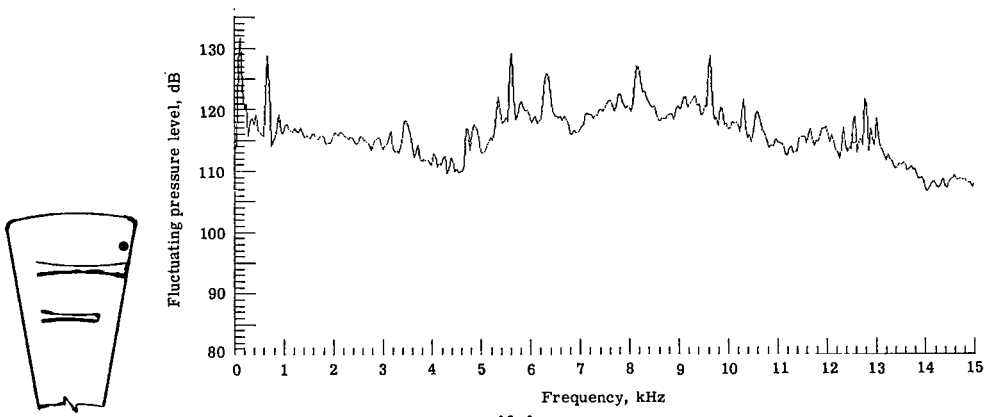


(b) FBMT H.

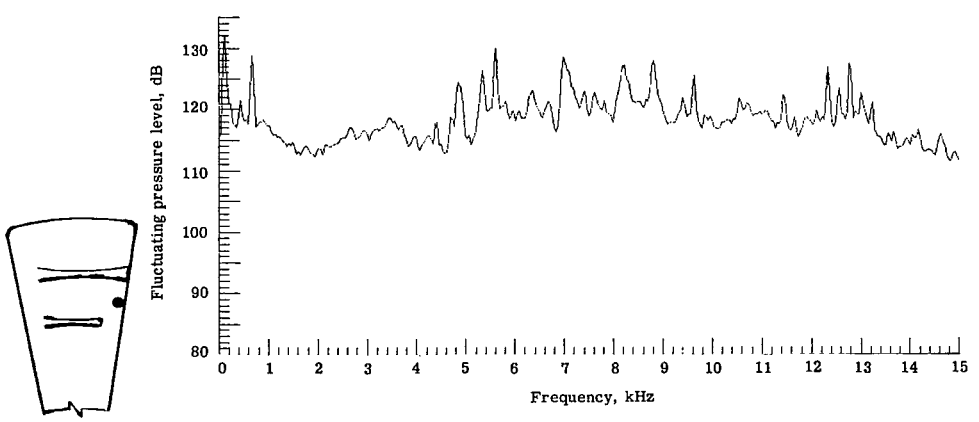


(c) FBMT G.

Figure 22.- Overall spectral plots for fan-blade-mounted transducers; 6750 rpm, 44 m/s tunnel speed.

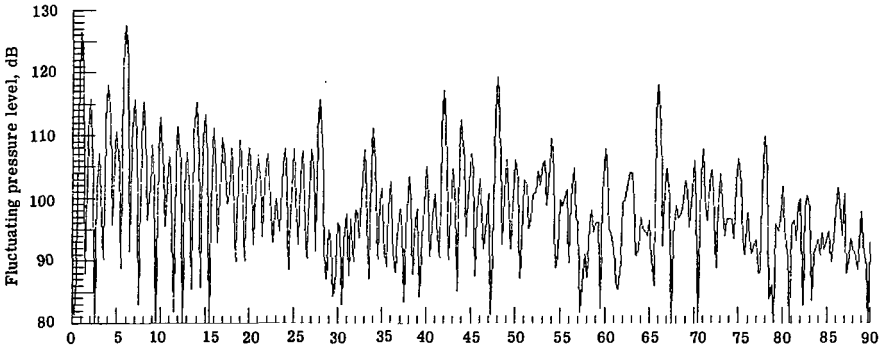


(a) FBMT I.

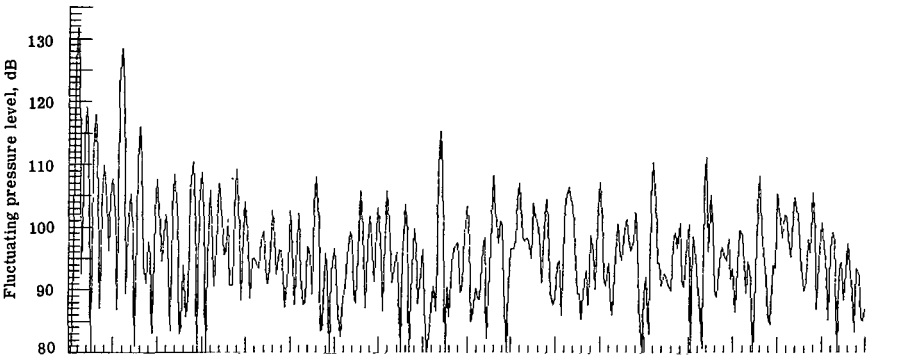


(b) FBMT H.

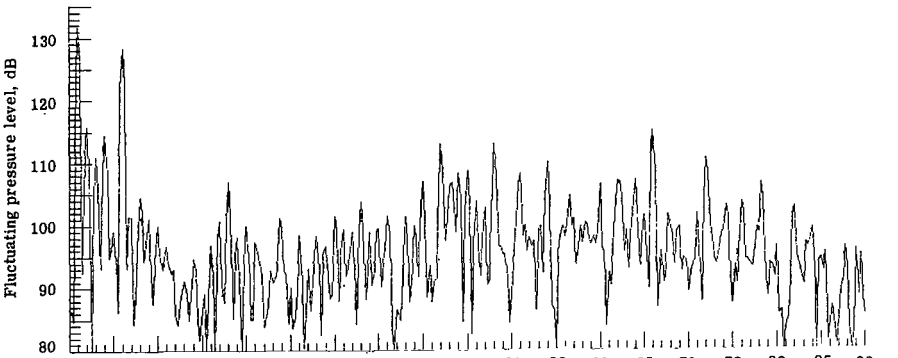


(c) FBMT G.

Figure 23.- Enhanced-signal spectral plots for fan-blade-mounted transducers; 6750 rpm, 44 m/s tunnel speed.

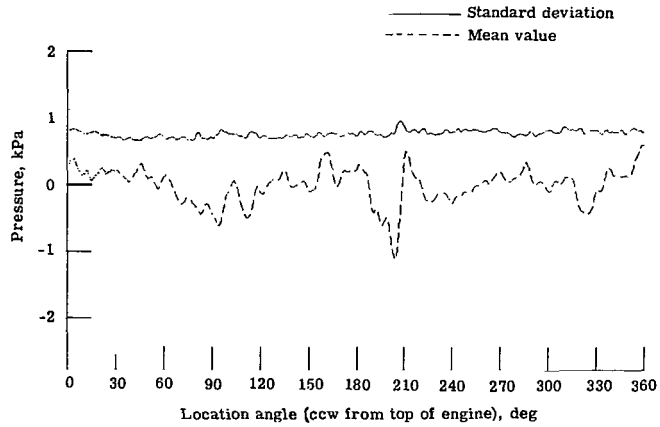


(a) FBMT I.

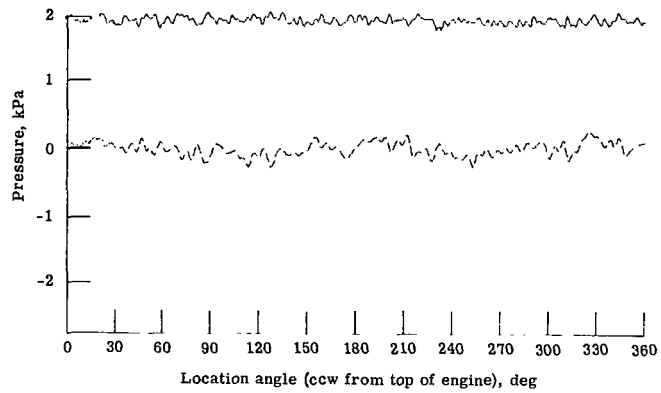


(b) FBMT H.

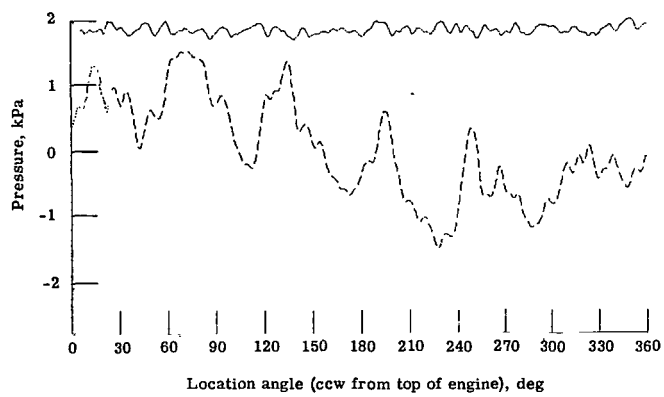


(c) FBMT G.

Figure 24.- Standard-deviation and mean-value plots for fan-blade-mounted transducers; 13 460 rpm, tunnel off.

| 1. Report No. | 2. Government Accession No. | 3. Recipient's Catalog No. |
|---|---|---|
| NASA TP-1976 | | |

| 4. Title and Subtitle | 5. Report Date |
|---|---|
| FLUCTUATING PRESSURES ON FAN BLADES OF A TURBOFAN ENGINE - STATIC AND WIND-TUNNEL INVESTIGATIONS | March 1982 |
| | 6. Performing Organization Code: 505-32-03-04 |
| 7. Author(s): James A. Schoenster | 8. Performing Organization Report No.: L-14913 |
| | 10. Work Unit No. |
| 9. Performing Organization Name and Address: NASA Langley Research Center, Hampton, VA 23665 | 11. Contract or Grant No. |
| | 13. Type of Report and Period Covered: Technical Paper |
| 12. Sponsoring Agency Name and Address: National Aeronautics and Space Administration, Washington, DC 20546 | 14. Sponsoring Agency Code |

15. Supplementary Notes

16. Abstract

As part of a program to investigate the fan noise generated from turbofan engines, miniature pressure transducers were used to measure the fluctuating pressure on the fan blades of a JT15D engine. Tests were conducted with the engine operating on an outdoor test stand and in a wind tunnel. It was found that a potential flow interaction between the fan blades and six, large support struts in the bypass duct is a dominate noise source in the JT15D engine. Effects of varying fan speed and the forward speed on the blade pressure are also presented.

| 17. Key Words (Suggested by Author(s)) | 18. Distribution Statement |
|---|---|
| Turbo-fan noise sources<br>Fan-blade-mounted pressure transducers<br>Static and wind-tunnel fan noise testing<br>Turbofan inlet turbulence | Unclassified - Unlimited<br><br>Subject Category 71 |

| 19. Security Classif. (of this report) | 20. Security Classif. (of this page) | 21. No. of Pages | 22. Price |
|---|---|---|---|
| Unclassified | Unclassified | 47 | A03 |

For sale by the National Technical Information Service, Springfield, Virginia 22161

NASA-Langley, 1982

National Aeronautics and
Space Administration

Washington, D.C.
20546

Official Business
Penalty for Private Use, $300

THIRD-CLASS BULK RATE

Postage and Fees Paid
National Aeronautics and
Space Administration
NASA-451


[illegible] 031662 S00030
DEPT OF THE AIR FORCE
AF WEAPONS LABORATORY
ATTN: TECHNICAL LIBRARY (SUL)
KIRTLAND AFB [illegible] 87117

NASA

POSTMASTER: If Undeliverable (Section 158 Postal Manual) Do Not Return